

## REFERENCES

- Ajaikumar, S., Golets, M., Larsson, L., Shchukarev, S., Kordas, K., Leino, A.R., and Mikkola, J.P. (2013). Effective dispersion of Au and Au–M (M = Co, Ni, Cu and Zn) bimetallic nanoparticles over TiO<sub>2</sub> grafted SBA-15: Their catalytic activity on dehydroisomerization of  $\alpha$ -pinene. Microporous and Mesoporous Materials, 173, 99–111.
- Almuhammed, S., Khenoussi, N., Bonne, M., Schacher, L., Lebeau, B., Adolphe, D., and Jocelyne Brendlé, J. (2014) Electrospinning of PAN nanofibers incorporating SBA-15-type ordered mesoporous silica particles. European Polymer Journal, 54, 71–78.
- Antoniou, N., Stavropoulos, G., and Zabaniotou, A. (2014) Activation of end of life tyres pyrolytic char for enhancing viability of pyrolysis-Critical review, analysis and recommendations for a hybrid dual system. Renewable and Sustainable Energy Reviews, 39, 1053-1073.
- Bandosz, T.J., Loureiro, J.M., and Kartel, M.T. (2006) Carbonaceous materials as desulfurization media: combined and hybrid adsorbents: Fundamentals and applications in NATO security through science series-C: Environmental security (pp. 145–64). The Netherlands: Springer.
- Belhakem, A. and Bengueddach, A. (2006) Catalytic properties and acidity of modified MCM-41 mesoporous materials with low Si/Al ratio: Hapane isomerization. Bulletin of the Chemical Society of Ethiopia, 20(1), 99-112.
- Bernardo, M., Lapa, N., Goncalves, M., Mendes, B., and Pinto, F. (2012) Study of the organic extraction and acidic leaching of chars obtained in the pyrolysis of plastics, tire rubber and forestry biomass wastes. Procedia Engineering, 42, 1739-1746.
- Bird, R.B., Stewart, W.E., and Lighfoot, E.N. (2007) Transport Phenomena. Rev. 2 nd ed., New York: John Wiley.
- Boxieng, S., Chunfei, W., Rui, W., Binbin, G., and Cai, L. (2006) Pyrolysis of waste tyres with zeolite USY and ZSM-5 catalyst. Applied Catalysis B: Environmental, 73, 150-157.

- Bunthid, D., Prasassarakich, P., and Hinchiranan, N. (2010) Oxidative desulfurization of tire pyrolysis naphtha in formic acid/H<sub>2</sub>O<sub>2</sub>/pyrolysis char system. Fuel, 89, 2617–2622.
- Byambajav, E. and Ohtsuka, Y. (2003) Cracking behavior of asphaltene in the presence of iron catalysts supported on mesoporous molecular sieve with different pore diameters. Fuel, 82, 1571–1577.
- Cao, Q., Jin, L., Bao, W., and Lv., Y. (2009) Investigations into the characteristics of oils produced from co-pyrolysis of biomass and tire. Fuel Processing Technology, 90, 337-342.
- Carrott, R.M.M.L., Candias, A.J.E., Carrott, P.J.M., Ravikovitch, P.I., Neimark, A.V., and Sequeira, A.D. (2001) Adsorption of nitrogen, neopentane, n-hexane, benzene and methanol for the evaluation of pore size in silica grades of MCM-41. Microporous and Mesoporous Materials, 47, 323-337.
- Čejka, J. (2004) Zeolites: Structures and inclusion properties. Encyclopedia of Supramolecular Chemistry, 2, 1623-1630.
- Cesarino, I., Marino, G., Matos, J.D.R., and Cavalheiro, E.T.G. (2007) Using the organofunctionalised SBA-15 nanostructured silica as a carbon paste electrode modifier: determination of cadmium ions by differential anodic pulse stripping voltammetry. Journal of the Brazilian Chemical Society, 18(4), 810-817.
- Chen, F. and Qian, J. (2002) Studies on the thermal degradation of cis-1,4-polyisoprene. Fuel, 81, 2071–2077.
- Chena, F., Huang, L., Yanga, X., and Wang, Z. (2013) Synthesis of Al-substituted MCM-41 and MCM-48 solid acids. Materials Letters, 109, 299–301.
- Cheng, X., Zhao, T., Fu, X., and Hu, Z. (2004) Identification of nitrogen compounds in RFCC diesel oil by mass spectrometry. Fuel Processing Technology, 85, 1463-1472.
- Chingombe, P., Saha, B., and Wakeman, R.J. (2005) Surface modification and characterization of a coal-based activated carbon. Carbon, 43, 3132-3143.

- Choi, S.S. (2000) Characterization of bound rubber of filled styrene-butadiene rubber compounds using pyrolysis-gas chromatography. Journal of Analytical and Applied Pyrolysis, 55, 161–170.
- Choi, J.S., Kim, D.J., Chang, S.H., and Ahn, W.S. (2003) Catalytic applications of MCM-41 with different pore sizes in selected liquid phase reactions. Applied Catalysis A: General, 254, 225–237.
- Choi, G.G., Jung, S.H., Oh, S.J., and Kim, J.S. (2014) Total utilization of waste tire rubber through pyrolysis to oils and CO<sub>2</sub> activation of pyrolysis char. Fuel Proceeding Technology, 123, 57-64.
- Choma, J. and Jaroniec, M. (2007) Applicability of classical methods of pore size analysis for MCM-41 and SBA-15 silicas. Applied Surface Science, 253, 5587–5590.
- Daehler, A., Boskovic, S., Gee, M.L., O'Connor, A.J., Separovic, F., and Stevens, G.W. (2005) Postsynthesis vapor-phase functionalization of MCM-48 with hexamethyldisilazane and 3-aminopropyldimethylethoxysilane for bioseparation applications. Journal Physical Chemistry, 109(1), 16263-16271.
- Dijkmans, T., Djokic, M.R., Geem, K.M.V., and Marin, G.B. (2015) Comprehensive compositional analysis of sulfur and nitrogen containing compounds in shale oil using GCxGC-FID/SCD/NCD/TOF-MS. Fuel, 140, 398-406.
- Du, H., Fairbridge, C., Yang, H., and Ring, Z. (2005) The chemistry of selective ring-opening catalysts. Applied Catalysis A: General, 294(1), 1-21.
- Dũng, N.A., Klaewkla, R., Wongkasemjit, S., and Jitkarnka, S. (2009) Light olefins and light oil production from catalytic pyrolysis of waste tire. Journal of Analytical and Applied Pyrolysis, 86, 281–286.
- Dũng, N.A., Wongkasemjit, S., and Jitkarnka, S. (2009) Effects of pyrolysis temperature and Pt-loaded catalysts on polar-aromatic content in tire-derived oil. Applied Catalysis, 91, 300-307.

- Flego, C. and Zannoni, C. (2011) N-containing species in crude oil fractions: An identification and qualification method by comprehensive two-dimensional gas chromatography coupled with quadrupole mass spectrometry. Fuel, 90, 2863-2869.
- Gobara, H.M. (2012) Characterization and catalytic activity of NiO/mesoporous aluminosilicate AISBA-15 in conversion of some hydrocarbons. Egyptian Journal of Petroleum, 21, 1-10.
- Gokce, Y. and Aktas, Z. (2014) Nitric acid modification of activated carbon produced from waste tea and adsorption of methylene blue and phenol. Applied Surface Science, 131, 352-359.
- Han, B., Zhang, F., Feng, Z., Liu, S., Deng, S., Wang, Y., and Wang, Y. (2014) A designed  $Mn_2O_3$ /MCM-41 nanoporous composite for methylene blue and rhodamine B removal with high efficiency. Ceramics International, 40, 8093–8101.
- Helleur, R., Popovic, N., Ikura, M., Stanculescu, M., and Liu D. (2001) Characterization and potential applications of pyrolytic char from ablative pyrolysis of used tires. Journal of Analytical and Applied Pyrolysis, 58, 813-824.
- International Union of Pure and Applied Chemistry. "IUPAC." 1997. 1 Jan 2015. <<http://www.iupac.org/>>
- Israel, G.D. (2013) Determining Sample Size. Florida: University of Florida.
- Jae, J., Tompsett, G.A., Foster, A.J., Hammond, K.D., Auerbach, S.M., Lobo, R.L., and Huber, G.W. (2011) Investigation into the shape selectivity of zeolite catalysts for biomass conversion. Journal of Catalyst, 279, 257-268.
- Jin, S., Cui, K., Guan, H., Yang, M., Liu, L., and Lan, C. (2012) Preparation of mesoporous MCM-41 from natural sepiolite and its catalytic activity of cracking waste polystyrene plastics. Applied Clay Science, 56, 1–6.
- Jiménez-Cruz, F. and Laredo, G.C. (2004) Molecular size evaluation of linear and branched paraffins from the gasoline pool by DFT quantum chemical calculations. Fuel, 83, 2183-2188.

- Johansson, E.M., Córdoba, J.M., and Odén, M. (2009) Synthesis and characterization of large mesoporous silica SBA-15 sheets with ordered accessible 18 nm pores. Mater Letter, 63, 2129–31.
- Jung, J.S., Park, J.W., and Seo, G. (2005) Catalytic cracking of n-octane over alkali-treated MFI zeolites. Applied Catalysis A: General, 288, 149–157.
- Kartini, I., Meredith, P., Da-Costa J.C.D., Riches, J.D., Lu, G.Q.M. (2004) Formation of mesostructured titania thin films using isopropoxide precursors. Current Apply Physics, 4, 160–2.
- Kibombo, H.S., Balasanthiran, V., Wu, C.M., Peng, R., and Koodali, R.T. (2014) Explration of room temperature synthesis of palladium containing cubic MCM-48 mesoporous materials. Microporous and Mesoporous Materials, 198, 1-8.
- Kirik, S.D., Parfenov, V.A., and Zharkov, S.M. (2014) Monitoring MCM-41 synthesis by X-ray mesostructure analysis. Microporous and Mesoporous Materials, 195, 21–30.
- Kresge, C.T., Leonowicz, M.E., Roth, W.J., Vartuli, J.C., and Beck, J.S. (1992) Ordered mesoporous molecular sieves synthesized by a liquid-crystal template mechanism. Nature, 359, 710–2.
- Kruk, M., Jaroniec, M., and Sayari, A. (2000) New insights into pore-size expansion of mesoporous silicates using long-chain amines. Microporous and Mesoporous Materials, 35-36, 545-553.
- Kwak, K.Y., Kim, M.S., Lee, D.W., Cho, Y.H., Han, J., Kwon, T.S., and Lee, K.Y. (2014) Synthesis of cyclopentadiene trimer (tricyclopentadiene) over zeolites and Al-MCM-41: The effects of pore size and acidity. Fuel, 137, 203-236.
- Laredo, G.C., Likhanova, N.V., Lijanova, I.V., and Rodriguez-Heredia, B. (2015) Synthesis of ionic liquids and their use for extracting nitrogen compounds from gas oil feeds towards diesel fuel production. Fuel Processing Technology, 130, 38-45.

- Lin, J., Zhao, B., Cao, Y., Xu, H., Ma, S., Guo, M., Qiao, D., and Cao, Y. (2014) Rationally designed Fe-MCM-41 by protein size to enhance lipase immobilization, catalytic efficiency and performance. Applied Catalysis A: General, 478, 175–185.
- López, F.A., Centeno, T.A., García-Díaz, I., and Alguacil, F.J. (2013a) Textural and fuel characteristics of the chars produced by the pyrolysis of waste wood, and the properties of activated carbons prepared from them. Journal of Analytical and Applied Pyrolysis, 104, 551-558.
- López, F.A., Centeno, T.A., Rodríguez, O., and Alguacil, F.J. (2013b) Preparation and characterization of activated carbon from the char produced in the thermolysis of granulated scrap tyres. Journal of the Air and Waste Management Association, 63(5), 534-544.
- Lui, T., Li, Z., Li, W., Shi, C., and Wang, Y. (2013) Preparation and characterization of biomass carbon-based solid acid catalyst for the esterification of oleic acid with methanol. Bioresource Technology, 133, 618-621.
- Makrigianni, V., Gainnakas, A., Deligiannakis, Y., and Komstantinou, I. (2015) Adsorption of phenol and methylene blue from aqueous solutions by pyrolytic tire char: Equilibrium and kinetic studies. Journal of Environmental Chemical Engineering, 3, 574-582.
- Marcus, Y. (2003) Review Commentary: The sizes of molecules-revisited. Journal of Physical Organic Chemistry, 16, 398-408.
- Marcilla, A., Gomez-Siurana, A., Menargyes, S., Ruiz-Femenia, R., and Garcia-Quesada, J.C. (2005) Oxidative degradation of EVA copolymers in the presence of MCM-41. Journal of Analytical and Applied Pyrolysis, 76, 138-143.
- Marvin, L. and Poutama. (2000) Fundamental reactions of free radicals relevant. Journal of Analytical and Applied Pyrolysis, 54, 5-35.
- Matzke, M., Jess, A, and Litzow, U. (2015) Polar nitrogen-containing aromatic compounds as carriers of natural diesel lubricity. Fuel, 140, 770-777.

- Mehio, N., Dai, S., and Jiang, D. (2014) Quantum Mechanical Basis for Kinetic Diameters of Small Gaseous Molecules. Journal of Physical Chemistry, 118, 1150-1154.
- Meléndez-Ortiz, H.I., Perera-Mercado, Y., Mercado-Silva, J.A., Olevarés-Maldonado, Y., Castruita, G., and García-Cerda, L.A. (2014) Functionalization with amine-containing organosilane of mesoporous silica MCM-41 and MCM-48 obtained at room temperature. Ceramics International, 40, 9701-9707.
- Meng, X., Wang, Z., Zhang, R., Xu, C., Liu, Z., Wang, Y., and Guo, Q. (2013) Catalytic conversion of C<sub>4</sub> fraction for the production of light olefins and aromatics. Fuel Processing Technology, 116, 217-221.
- Midgley, T.J., and Henne, A.I. (1929) Naturalandsyntheticrubber I. product soft head structive distillation of natural rubber. Journal of the American Chemical Society, 51, 1215–1226.
- Miguel, G.S., Aguado, J., Serrano, D.P., and Escola, J.M. (2006) Thermal and catalytic conversion of used tyre rubber and its polymeric constituents using Py-GC/MS. Applied Catalysis B: Environmental, 64, 209–219.
- Mirmiran, S., Pakdel, H., and Roy, C. (1992) Characterization of used tire vacuum pyrolysis oil: nitrogenous compounds from the naphtha fraction. Journal of Analytical and Applied Pyrolysis, 22, 205-215.
- Muenpol, S., Yuwaporpanit, R., and Jitkarnka, S. (2015), Valuable petrochemicals, petroleum fractions, and sulfur compounds in oils derived from waste tyre pyrolysis using five commercial zeolites as catalysts: impact of zeolite properties. Clean Techn Environ Policy, DOI 10.1007/s10098-015-0935-8.
- Na, K., Choi, M., and Ryoo, R. (2013) Recent advances in the synthesis of hierarchically nanoporous zeolites. Microporous and Mesoporous Materials, 166, 3–19.
- Ng, E., Goh, J.Y., Ling, T.C., and Mukti, R.R. (2013) Eco-friendly synthesis for MCM-41 nanoporous materials using the non-reacted reagents in mother liquor. Nanoscale Research Letters, 8(1), 120.

- Nunes, M.A.G., Mello, P.A., Bizzi, C.A., Diehl, L.O., Moreira, E.M., Souza, W.F., Gaudino, E.C., Cravotto, G., and Flores, E.M.M. (2014) Evaluation of nitrogen effect on ultrasound-assisted oxidative desulfurization process. Fuel Processing Technology, 126, 521-527.
- Matzke, M., Jess, A, and Litzow, U. (2015) Polar nitrogen-containing aromatic compounds as carriers of natural diesel lubricity. Fuel, 140, 770-777.
- Mirmiran, S., Pakdel, H., and Roy, C. (1992) Characterization of used tire vacuum pyrolysis oil: nitrogenous compounds from the naphtha fraction. Journal of Analytical and Applied Pyrolysis, 22, 205-215.
- Oldenburg, T.B.P., Brown, M., Bennett, B, and Larter, S. R. (2014) The impact of thermal maturity level on the composition of crude oils, assessed using ultra-high resolution mass spectrometry. Organic Geochemistry, 75, 151-168.
- On-x Life Technologies, Inc. "On-X Pyrolytic Carbon." 2013. 10 May 2014. <<http://www.onxlti.com/product-divisions/contract-manufacturing-products/on-x-pyrolytic-carbon/>>
- Pirika. "Joback method." 1999. 20 October 2014 <[www.pirika.com/ENG/TCPE/HTML5/Joback/index.html](http://www.pirika.com/ENG/TCPE/HTML5/Joback/index.html)>
- Pithakratanayothin, S. (2014). Analysis of a tire-derived oil using GCxGC/TOF-MS for better identification and grouping of hydrocarbon compounds. M.S. Thesis, The Petroleum and Petrochemical Collage, Chulalongkorn University, Bangkok, Thailand.
- Pithakratanayothin, S. and Jitkarnka, S. (2014) Comparison of components in oil derived from tyre pyrolysis with and without KL catalyst using GCxGC/TOF-MS. Chemical Engineering Transaction, 39, 1261-126.
- Royal Society of Chemistry. "ChemSpider." 2015. 20 February 2015 <[www.ChemSpider.com](http://www.ChemSpider.com)>
- Seddegi, S.Z., Budrthumal, U., Al-Arfaj, A.A., Al-Amer, A.M., and Barri, S.A. (2002) Catalytic cracking of polyethylene over all-silica MCM-41 molecular sieve. Applied Catalysis A: General, 225, 167-176.



- Seng-eiad, S. and Jitkarnka, S. (2015) Estimation of average kinetic and maximum diameters of hydrocarbon groups in tyre-derived oil for catalyst design purpose. Chemical Engineering Transaction. (in press)
- Shi, B. and Que, G. (2003) Cracking and cracking selectivity of alkane and alkyl aromatics: effects of dispersed catalysis and hydrogen donors. American Chemical Society, 48(2), 631-633.
- Sim, A., Cho, Y., Kim, D., Witt, M., Birdwell, J.E., Kim, B.J., and Kim, S. (2015) Molecular-level characterization of crude oil compounds combining reversed-phase high-performance liquid chromatography with off-line high-resolution mass spectrometry. Fuel, 140, 717-723.
- Simpson, N.J.K. "Solid Phase Extraction." 2015. 20 March 2015 <<http://www.slideshare.net/RonaldTalvat/solid-phase-extraction-principles-techniques-and-application>>
- Soltani, S.M., Yazdi, S.K., Hosseini, S., and Gargari, M.K. (2014) Effect of nitric acid modification on porous characteristics of mesoporous char synthesized from the pyrolysis of used cigarette filters. Journal of Environmental Chemical Engineering, 2, 1301-1308.
- Tong, J., Liu, J., Han, X., Wang, S., and Jiang, X. (2013) Characterization of nitrogen-containing species in Huadian shale oil by electrospray ionization Fourier transform ion cyclotron resonance mass spectrometry. Fuel, 104, 365-371.
- Uhl, F.M., McKinney, M.A., and Wilkie, C.A. (2000) Polybutadiene cross-linked with various diols-effect on thermal stability. Polymer Degradation and Stability, 70, 417-424.
- University of Strathclyde "Sorbent Synthesis and Application." 2010. 5 May 2014 <[http://info.chem.strath.ac.uk/people/academic/lorraine\\_gibson/research/sorbents](http://info.chem.strath.ac.uk/people/academic/lorraine_gibson/research/sorbents)>
- Voegtlin A.C., Ruch F., Guth J.L., Patarin J., and Huve L. (1997) F<sup>-</sup>mediated synthesis of mesoporous silica with ionic- and non-ionic surfactants a new templating pathway. Micropore Mater, 9(1), 95-105.

- Wang, Y., Noguchi, M., Takahashi, Y., and Ohtsuka, Y. (2001) Synthesis of SBA-15 with different pore sizes and the utilization as supports of high loading of cobalt catalysts. Catalysis Today, 68, 3–9.
- Wei, Q., Wen, S., Tao, X., Zhang, T., Zhou, Y., Chung, K., and Chunming, X. (2015) Hydrodenitrogenation of basic and non-basic nitrogen-containing compounds in coker gas oil. Fuel Processing Technology, 129, 76-84.
- Wikipedia, “Pyrolysis carbon.” 2014. 10 May, 2014 <[http://en.wikipedia.org/wiki/Pyrolytic\\_carbon](http://en.wikipedia.org/wiki/Pyrolytic_carbon)>
- Williams, P.T. and Bottrill, R.P. (1995) Sulfur-polycyclic aromatic hydrocarbons in tyre pyrolysis oil. Fuel, 74, 736-42.
- Witpathomwong, C., Longloilert, R., Wongkasemjit, S., and Jitkarnka, S. (2011) Improving light olefins and light oil production using Ru/MCM-48 in catalytic pyrolysis of waste tire. Energy Procedia, 9, 245 – 25.
- Yang, P.D., Zhao, D.Y., Margolese, D.I., Chmelka, B.F., and Stucky, G.D. (1998) Generalized syntheses of large-pore mesoporous metal oxides with semicrystalline frameworks. Nature, 396, 152–5.
- Yu, G., Lu, S., Chen, H., and Zhu, Z. (2005) Diesel fuel desulfurization with hydrogen peroxide promoted by formic acid and catalyzed by activated carbon. Carbon, 43, 2285–94.
- Yuwapornpanit, R. and Jitkarnka, S. (2015) Cu-doped catalysts and their impacts on tire-derived oil and sulfur removal. Journal of Analytical and Applied Pyrolysis, 111, 200-208.
- Zhao, D.Y., Huo, Q.S., Feng, J.L., Chmelka, B.F., and Stucky, G.D. (1998). Nonionic triblock and star diblock copolymer and oligomeric surfactant syntheses of highly ordered, hydrothermally stable, mesoporous silica structures. Journal of the American Chemical Society, 120, 6024–36.

## APPENDICES

### Appendix A Estimation of Molecular Size

#### 1. Determination of Sampling Size

The hydrocarbon compounds which were detected in tire-derived oil using GCxGC-TOF/MS were selected the representative data by using Yamane method (Israel, 2013) as seen in Eq. (A1). Then, the representative molecules with a high percent area (high concentration) were considered. The examples of calculation were shown as followed.

$$n = \frac{N}{1 + N(e)^2}$$

Where  $n$  = Sampling size (species) (A1)

$N$  = Population of hydrocarbons in each group (species)

\* The population of hydrocarbons was obtained from  
GCxGC/TOF-MS

$e$  = 0.1 (assume 90 % confidence level)

Example: SATs population in non-catalysts case is 42 species

$$n = \frac{42}{1 + 42(0.1)^2} = 30 \text{ species}$$

So, the sampling size is 30 species.

Then, the species in each hydrocarbon group with high concentration were selected as the representative compounds as seen in Table A1.

**Table A1** Sampling size and representatives from each group of compounds

Molecular Group	Number of Detected Compounds					Number of Sampling Size <sup>a</sup>					%Area of Detected Compounds					%Area of Sampling				
	1	2	3	4	5	1	2	3	4	5	1	2	3	4	5	1	2	3	4	5
SATs	42	55	61	63	66	30	35	38	39	40	5.3	5.5	5.0	4.9	3.9	5.2	5.4	4.8	4.7	3.8
OLEs	110	106	129	128	129	52	51	56	56	56	7.4	7.4	10.5	9.1	8.1	6.2	6.5	9.6	8.0	7.1
NAPs	42	64	96	80	86	30	39	49	44	46	2.0	3.2	4.1	3.4	3.8	1.9	3.0	3.8	3.0	3.5
TERs	100	109	143	146	151	50	52	59	59	60	6.7	6.5	8.9	10.5	11.4	5.8	5.7	7.5	9.1	10.1
MAHs	231	203	240	248	213	70	67	71	71	68	46.9	59.1	53.5	55.3	56.7	40.6	50.0	45.9	45.9	49.1
DAHs	27	16	25	25	25	21	14	20	20	20	9.2	4.0	4.1	3.6	3.7	9.2	4.0	4.1	3.6	3.7
PAHs	96	72	93	104	95	49	42	48	51	49	12.1	8.5	6.9	8.5	6.3	11.2	8.0	6.5	7.9	6.1
PPAHs	174	141	193	115	140	64	59	66	53	58	10.4	5.7	7.1	4.8	6.0	9.0	5.2	6.3	4.5	5.8
Total	822	766	980	909	905	365	359	407	394	398	100	100	100	100	100	89.0	87.7	88.4	86.8	89.0

<sup>a</sup> Yamane (Israel, 2013)

1 = non-catalyst, 2 = Al-MCM-41, 3 = Al-SBA-15, 3 = Si-MCM-41, 4 = Si-MCM-48

## 2. Determination of Molecular Diameters

There are two methods for molecular diameter estimation; that are, kinetic diameter ( $\varnothing_k$ ) and maximum diameter ( $\varnothing_m$ ) as seen in Eq. (A2) and Eq. (A3), respectively. The kinetic diameter of molecule is defined as the molecular diameter during movement whereas the maximum diameter of molecule is defined as the longest part of molecule.

### 2.1 Kinetic Diameter (Bird *et al.* 2007; Jae *et al.* 2011)

$$\varnothing_k = 0.84V_C^{\frac{1}{3}} \quad (\text{A2})$$

Where  $\varnothing_k$  = Kinetic diameter (Å)  
 $V_c$  = Critical volume (cm<sup>3</sup>/mol)

Note: The critical volume was manually calculated according to the functional group within molecular structure based on Joback method (Pirika, 1999).

Example:

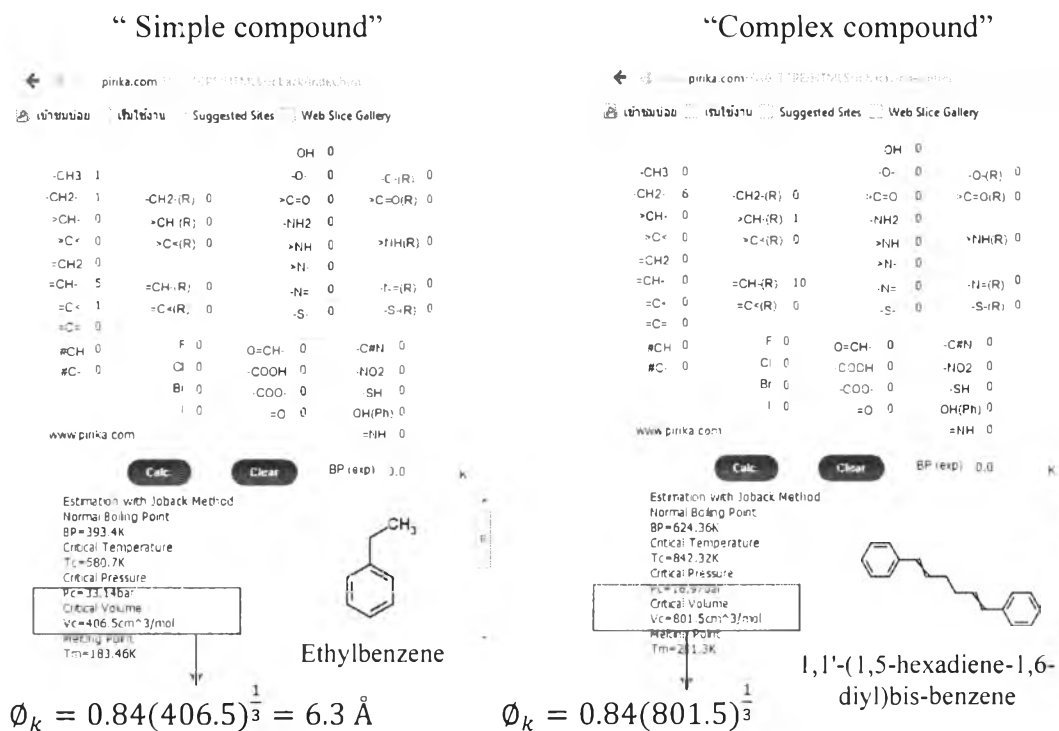


**Figure A1** Kinetic diameter of simple and complex compounds.

## 2.2 Maximum diameter (Royal Society of Chemistry, 2015)

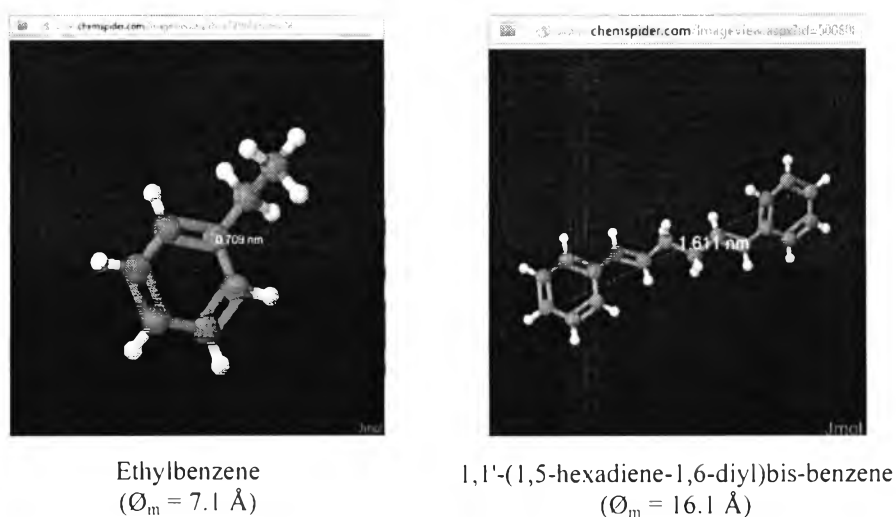


**Figure A2** Maximum diameter of simple and complex compounds.

**Table A2** Ranges of molecular size in each hydrocarbon group

Groups of Components	Small Size (< 8 Å)			Medium Size (8-16 Å)			Large Size (> 16 Å)		
	1	2	3	1	2	3	1	2	3
SATs	-	7.6	6.3	8.7-15.9	9.6-15.1	9.6-15.3	16.2-34.7	16.0-34.7	16-34.7
OLEs	6.6-7.7	7.3	6.6-7.7	8.1-15.8	8.1-15.9	8.1-15.7	16.7-22.6	16.0-28.2	16.2-28.2
NAPs	5.9-7.9	6.6-7.7	4.8-7.9	8.0-13.9	8.0-13.4	8.0-13.3	-	-	-
TERs	5.7-7.9	6.7-7.8	5.0-7.9	8.0-12.6	8.0-12.6	8.0-14.5	-	-	-
MAHs	6.2-7.9	5.9-7.9	5.5-7.9	8.0-14.4	8.0-13.2	8.0-13.2	-	-	-
DAHs	7.1-7.6	7.0-7.6	7.1-7.5	8.1-15.6	8.1-9.3	8.0-11.6	-	-	-
PAHs	7.6	-	-	8.4-15.1	8.2-15.1	8.2-15.1	16.1	16.1	-
PPAHs	5.5-7.9	5.5-7.9	5.2-7.9	8.2-15.4	8.1-14.8	8.2-15.4	16.7	-	-

1 = Non-catalyst, 2 = Al-MCM-41, 3 = Al-SBA-15

**Table A3** Concentration of molecules in each hydrocarbon group

Groups of components	Small Size (< 8 Å)			Medium Size (8-16 Å)			Large Size (> 16 Å)		
	1	2	3	1	2	3	1	2	3
SATs	0.00	0.3	0.0	2.0	2.5	2.7	3.8	3.5	2.9
OLEs	0.2	0.1	0.6	5.2	5.8	9.3	1.5	1.7	1.3
NAPs	0.7	1.5	2.0	1.5	1.4	2.3	0.0	0.0	0.0
TERs	3.0	4.3	4.0	3.5	2.1	4.7	0.0	0.0	0.0
MAHs	19.9	34.0	27.7	25.7	24.1	25.6	0.0	0.0	0.0
DAHs	6.8	2.5	0.1	3.5	2.1	4.6	0.0	0.0	0.0
PAHs	0.0	0.0	0.0	0.1	9.2	7.5	12.4	0.1	0.0
PPAHs	11.1	2.6	1.4	5.1	2.3	3.4	3.9	0.0	0.0

1 = Non-catalyst, 2 = Al-MCM-41, 3 = Al-SBA-15

### 3. Average Size of Molecules

The area percentages of sampling species were normalized, and the distribution of kinetic and maximum diameters of each molecular group were plotted with the increment 0.5 Å, in order to calculate the average molecular sizes from the distributions as seen in Figure A3.

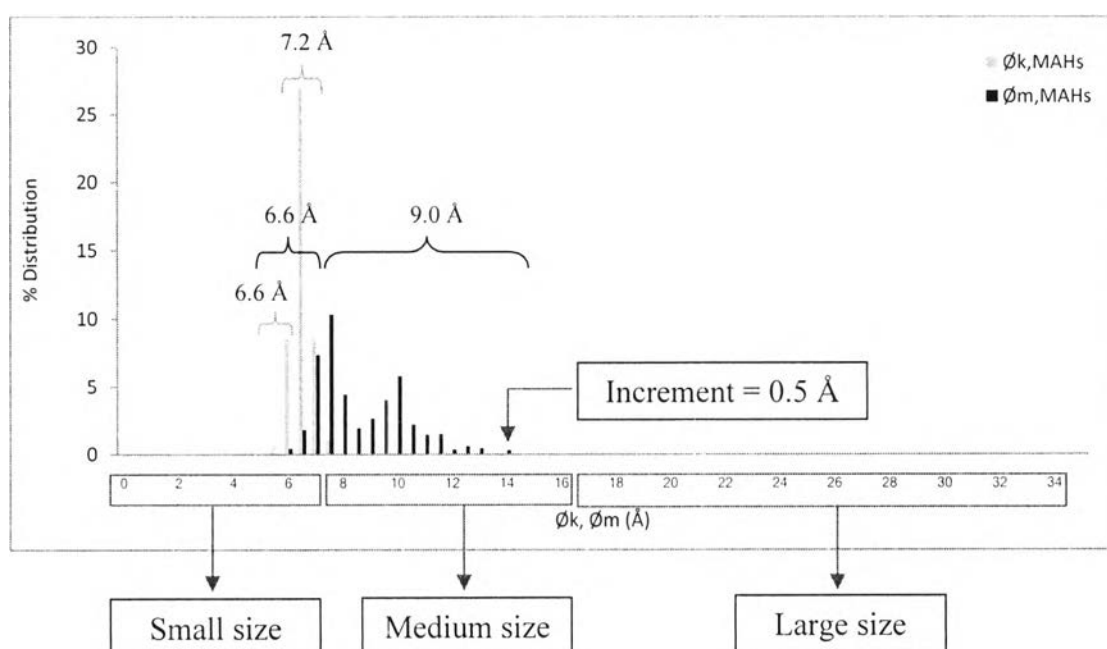


**Figure A3** Molecular size distributions of components in mono-aromatics (MAHs).

The average kinetic and average maximum diameters in each distribution range were subsequently determined using Eq. (A3), where  $\omega$  and  $m$  are defined as the weight fraction of each species and the number of species in each range, respectively.

$$\phi_{avg} = \frac{\sum_{i=1}^m \omega_i \phi_i}{\sum_{i=1}^m \omega_i} \quad (A3)$$

Example: Calculation of average kinetic diameter ( $\bar{\phi}_{k,avg}$ ; Å)

Range: 6.0-6.9 Å (m = 50)

$$\begin{aligned}\bar{\phi}_{k,avg} &= \frac{\sum_{i=1}^m \omega_i \phi_{k,i}}{\sum_{i=1}^m \omega_i} \\ &= \frac{\sum_{i=1}^{50} (0.57(5.96) + 1.65(6.07) + 0.20(6.07) + \dots + 0.38(6.91) + 0.25(6.92) + 0.20(6.93))}{\sum_{i=1}^{50} (0.57 + 1.65 + 0.20 + \dots + 0.38 + 0.25 + 0.20)} \\ &= 6.6 \text{ Å}\end{aligned}$$

So, the average kinetic diameter in the range of 6.0-6.9 Å is 6.6 Å.

Example: Calculation of average maximum diameter ( $\bar{\phi}_{m,avg}$ ; Å)

Range: 8.0-14.4 Å (m = 65)

$$\begin{aligned}\bar{\phi}_{m,avg} &= \frac{\sum_{i=1}^m \omega_i \phi_{m,i}}{\sum_{i=1}^m \omega_i} \\ &= \frac{\sum_{i=1}^{65} (0.52(8.04) + 0.84(8.10) + 0.48(8.20) + \dots + 1.30(12.85) + 1.00(13.15) + 0.68(14.44))}{\sum_{i=1}^{65} (0.52 + 0.84 + 0.48 + \dots + 1.30 + 1.00 + 0.68)} \\ &= 9.0 \text{ Å}\end{aligned}$$

So, the average kinetic diameter in the range of 8.0-14.4 Å is 9.0 Å.

**Table A4** Average kinetic and maximum diameters of compositions in each group of non-catalyst case

Group of Components		Average Kinetic Diameter ( $\bar{\phi}_{k,avg}$ ; Å) <sup>a,b</sup>	Average Maximum Diameter ( $\bar{\phi}_{m,avg}$ ; Å) <sup>b,c</sup>		
			Small (< 8 Å)	Medium (8-16 Å)	Large (>16 Å)
MAHs	Range	6.0-6.9, 7.0-7.6	6.0-7.0	8.0-14.4	-
	Avg.	6.6, 7.2	6.6	9.0	-

<sup>a</sup>Eq(A2), <sup>b</sup>Eq(A3), and <sup>c</sup>(Royal Society of Chemistry, 2015)



#### 4. Distribution of all Molecular Size

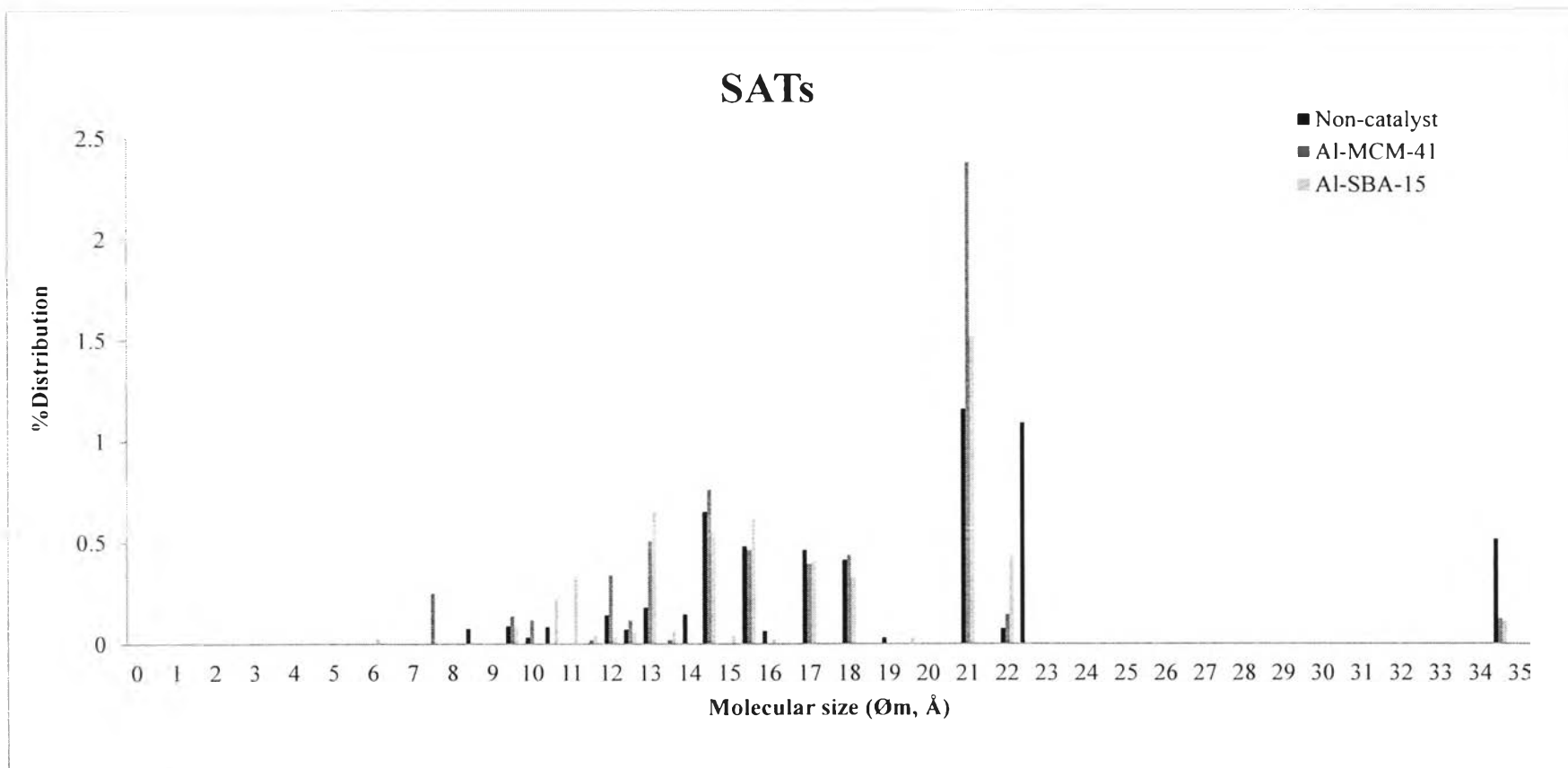


**Figure A4** Distribution of molecular size of saturated hydrocarbons (SATs).

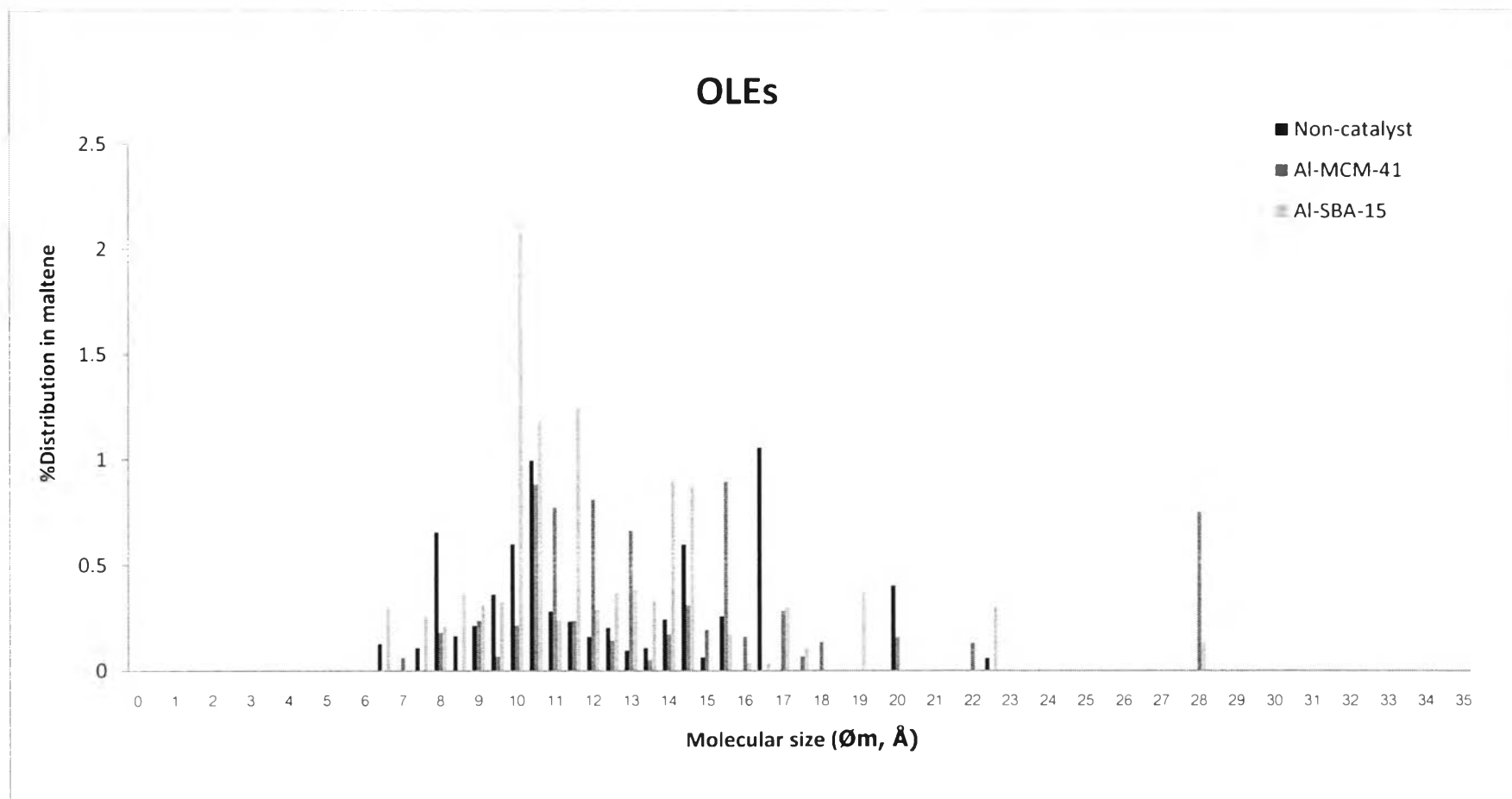
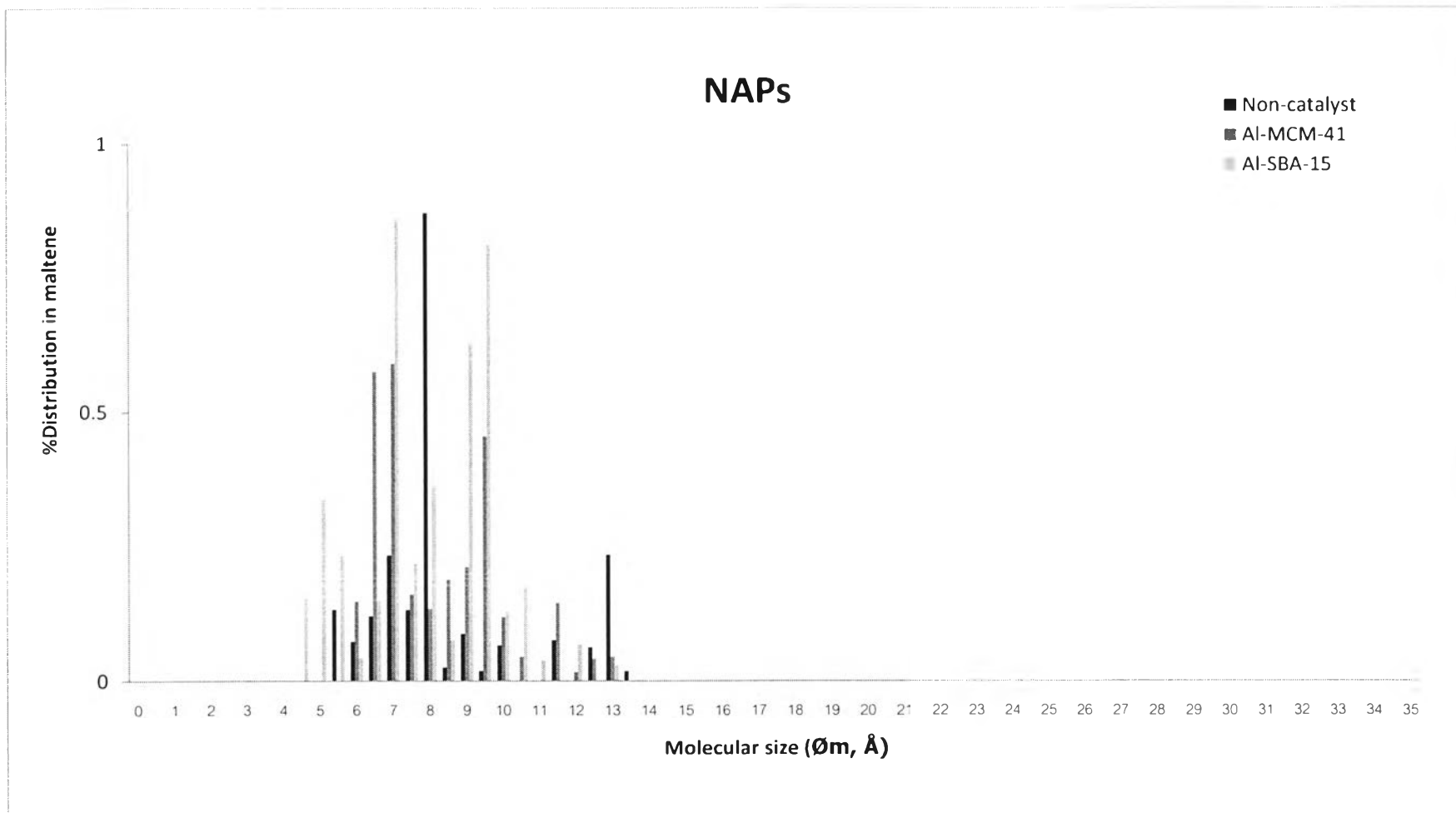
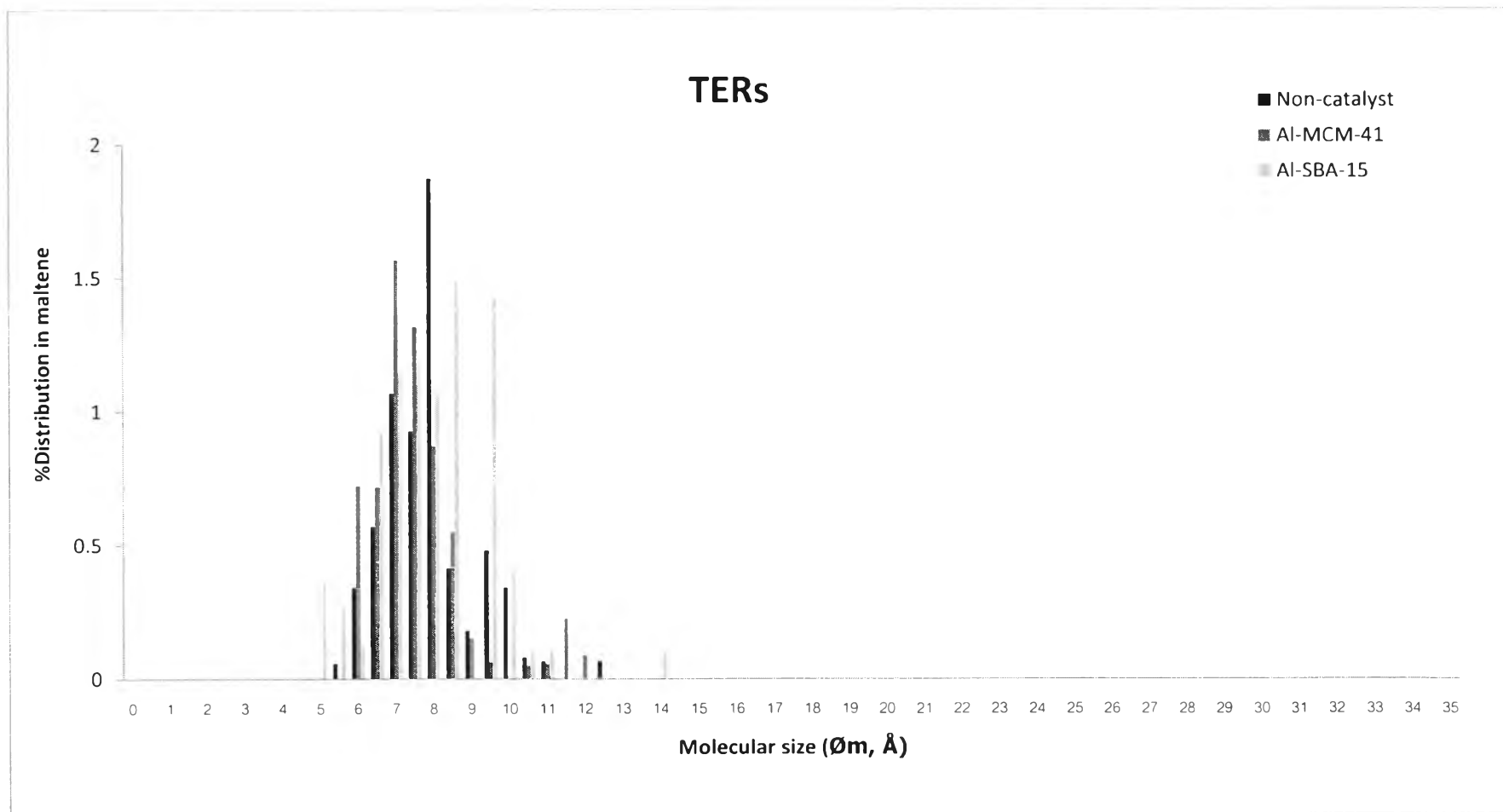


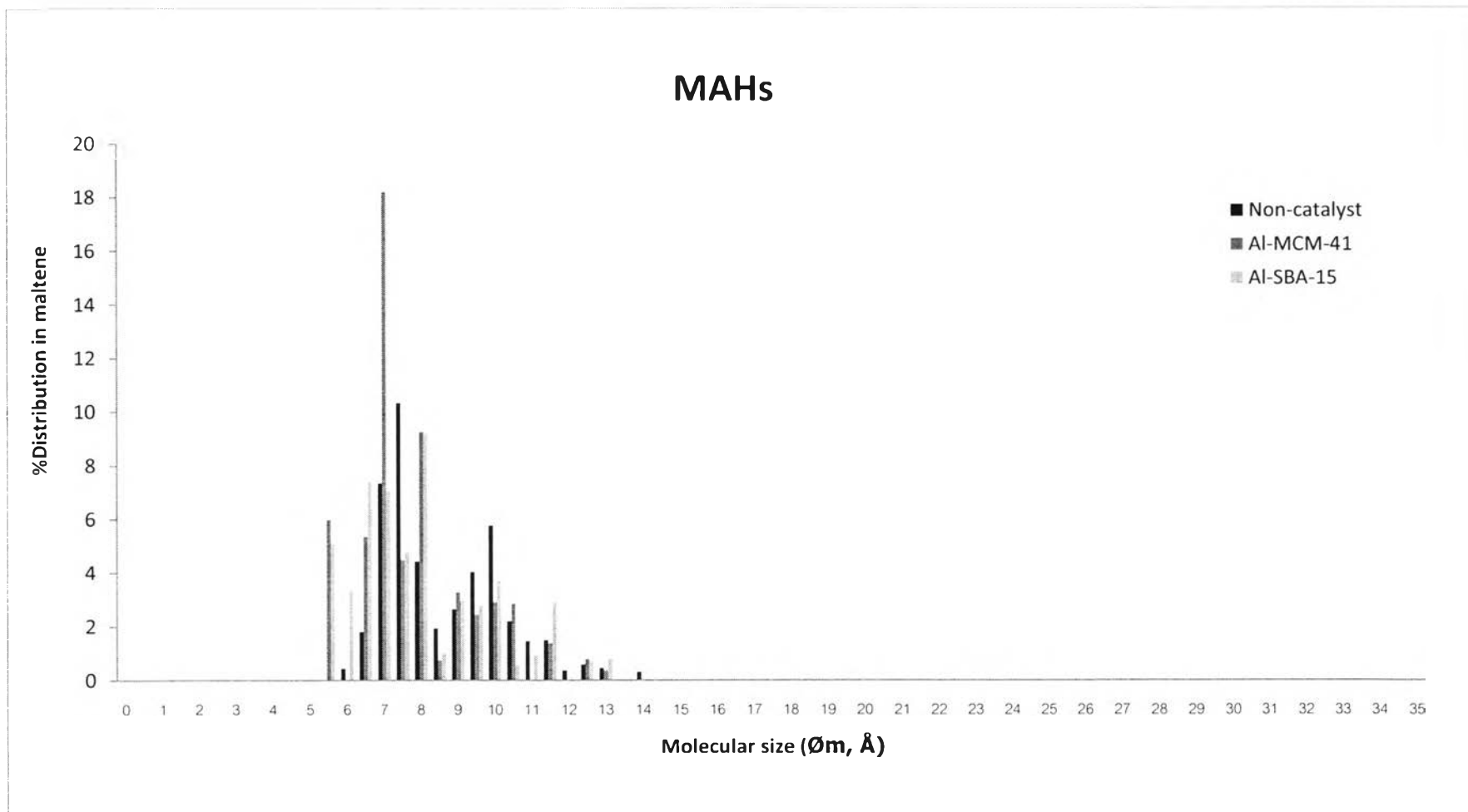
Figure A5 Distribution of molecular size of olefins (OLEs).



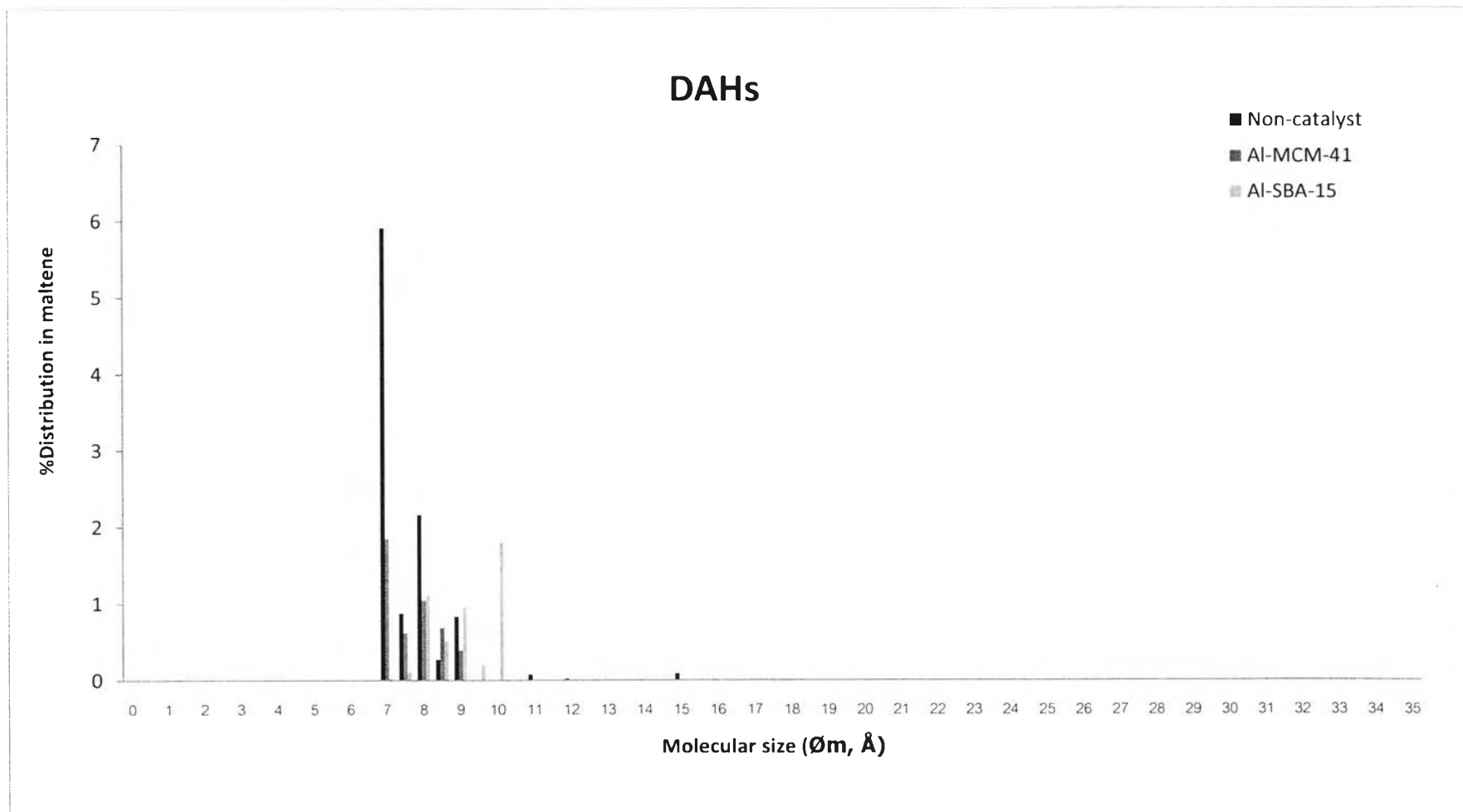
**Figure A6** Distribution of molecular size of naphthenes (NAPs).



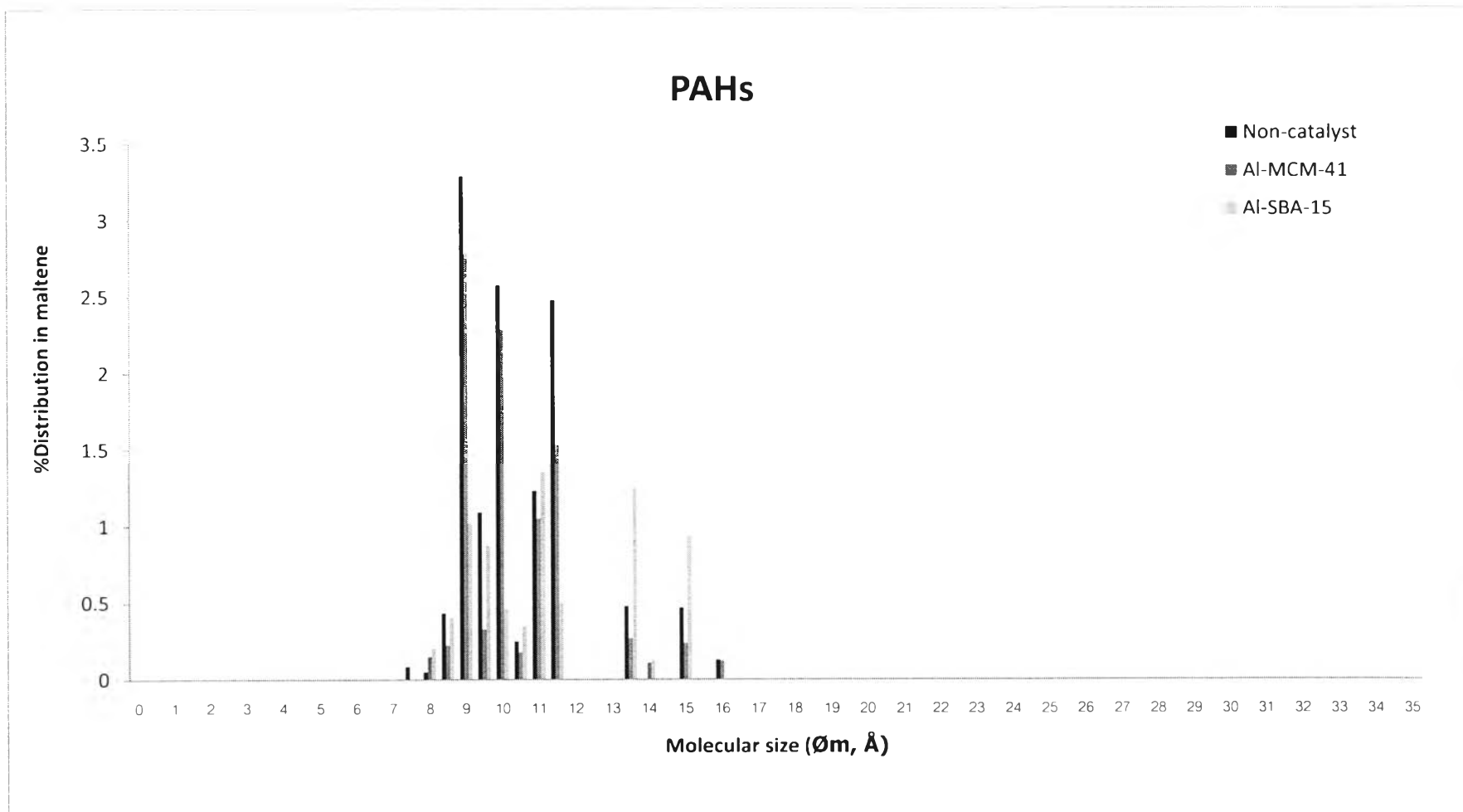
**Figure A7** Distribution of molecular size of terpenes (TERs).



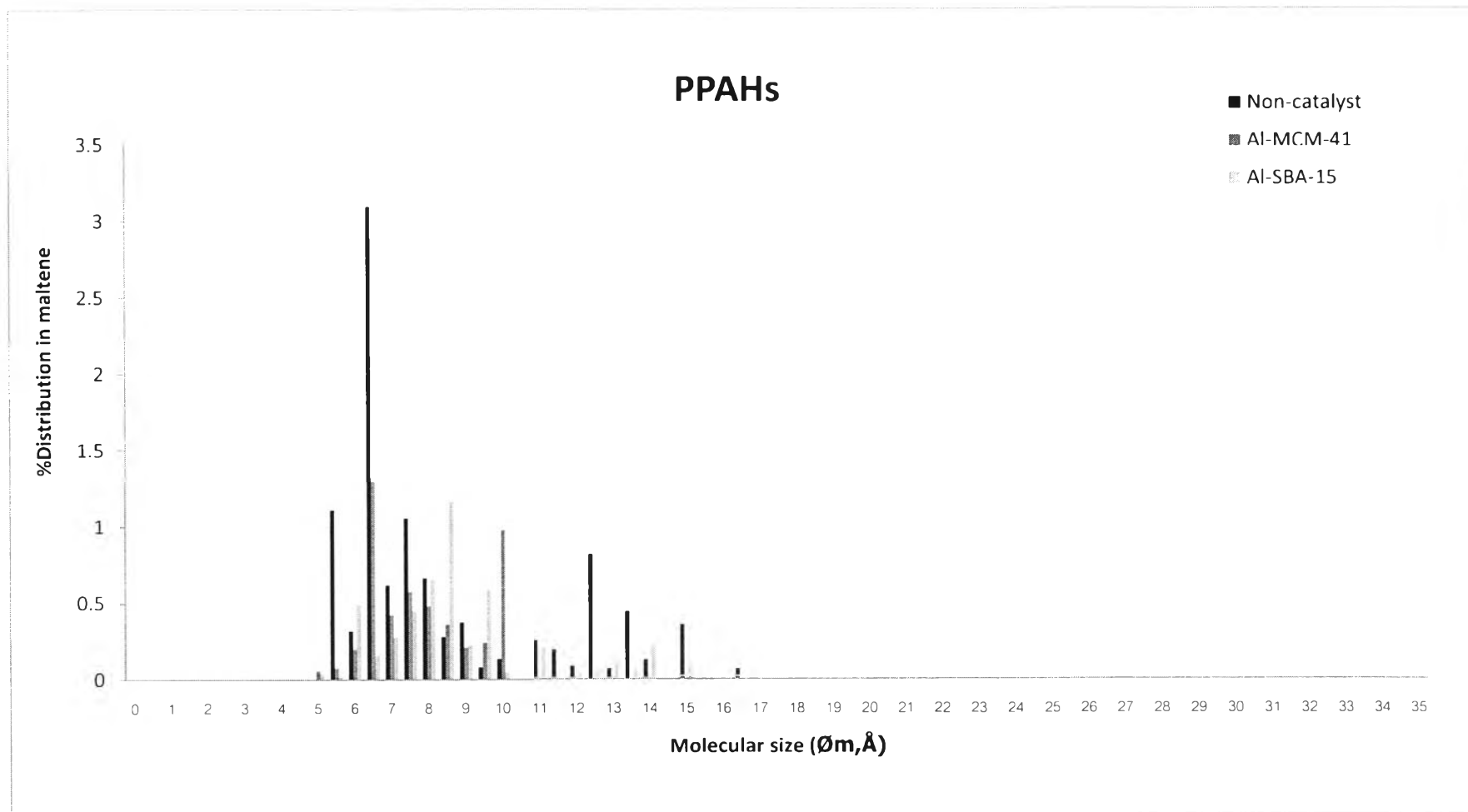
**Figure A8** Distribution of molecular size of mono-aromatics (MAHs).



**Figure A9** Distribution of molecular size of di-aromatics (DAHs).

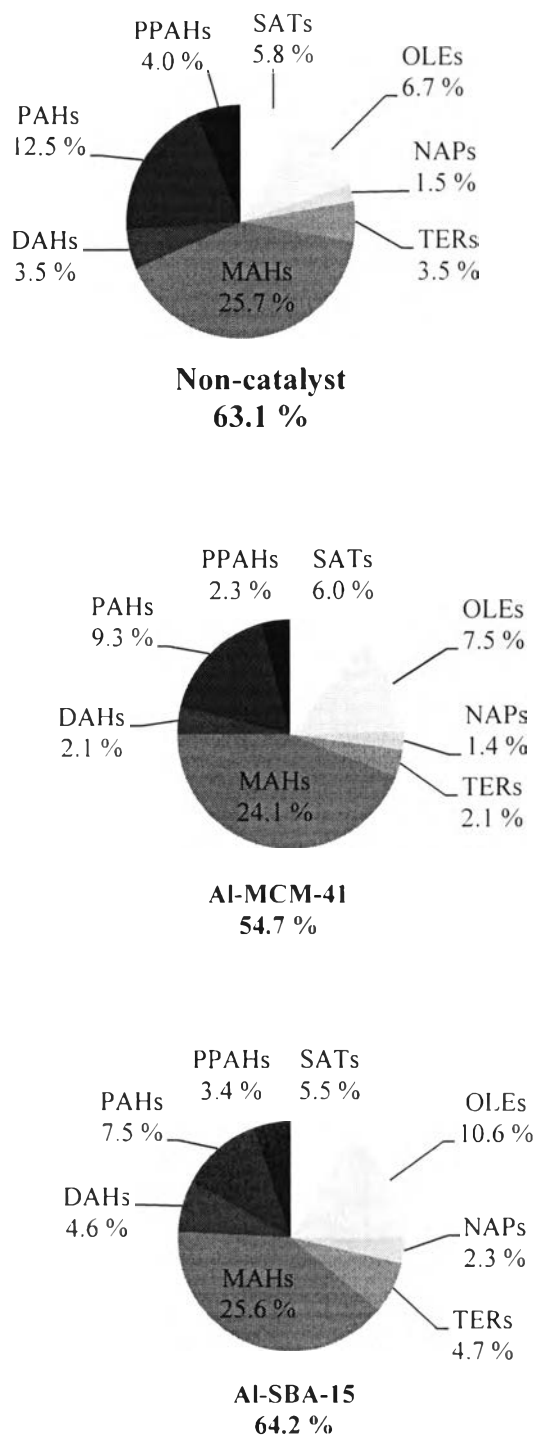


**Figure A10** Distribution of molecular size of poly-aromatics (PAHs).



**Figure A11** Distribution of molecular size of polar-aromatics (PPAHs).



5. Distribution of Large-molecular Size

**Figure A12** Distribution of large-size molecules (> 8 Å).

6. Distribution of Molecular Sizes of Compounds in Tire-derived Oil in all Petroleum Fractions

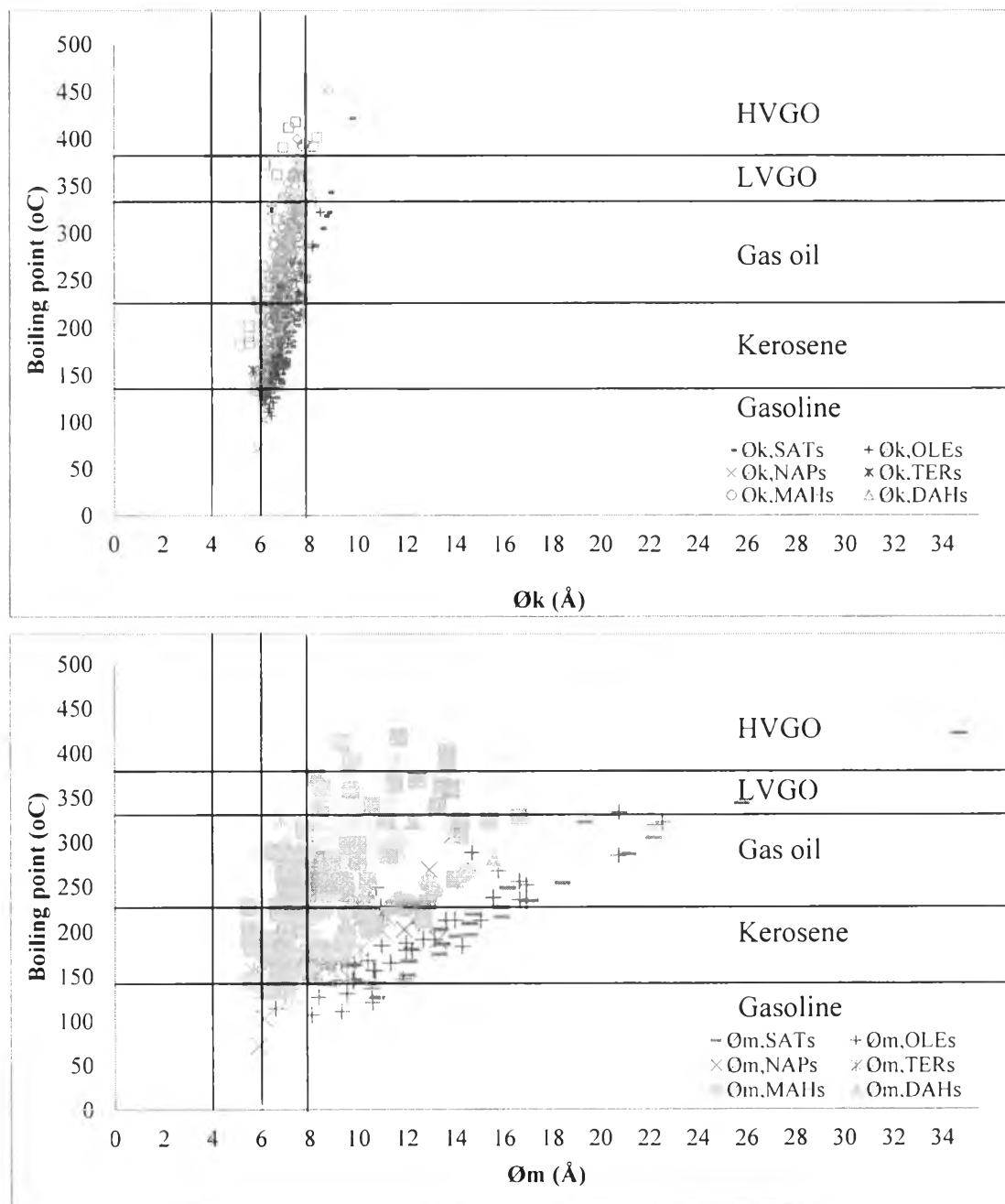


**Figure A13** Distribution of molecular sizes of compounds in tire-derived oil in all petroleum fractions obtain from non-catalyst case: (a) kinetic diameter ( $\text{Ø}_k$ ) and (b) maximum diameter ( $\text{Ø}_m$ ).

## Appendix B Overall Yields of Pyrolysis Products

**Table B1** Yield of products

Scope	Catalyst	Product Distribution (wt%) <sup>a</sup>			
		Gas	Liquid	Solid	Coke
	Non-catalyst	13.23	41.09	45.68	0.00
Pore Size	Al-MCM-41	9.30	41.48	43.61	5.61
	Al-SBA-15	13.16	40.41	43.21	3.23
Pore Structure	Si-MCM-41	9.55	42.41	43.13	4.90
	Si-MCM-48	11.64	38.91	43.67	5.79
Pyrolysis Char	Untreated Char	13.21	40.84	45.03	0.93
	5 M HNO <sub>3</sub> -treated Char	14.53	38.41	44.97	2.09

<sup>a</sup> Mass balance

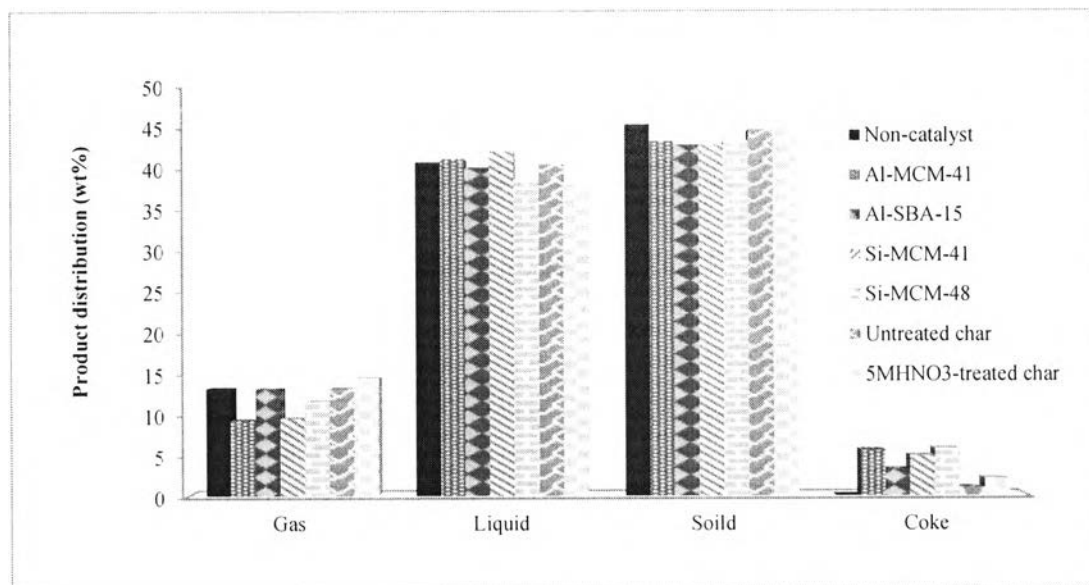


**Figure B1** Product distribution.

## Appendix C Gas Products

### 1. Calculation of response factors ( $f_i$ ) of gases

The response factors were calculated on the weight basis using methane as the standard. The mass of each gas component ( $G_i$ ) was calculated using Eq. (C1) and then the response factor of each gas component was calculated using Eq. (C2).

$$G_i = (4.0220 \times 10^{-7})(\%_i)(Mw_i) \quad (C1)$$

$$f_i = \left( \frac{A_{std}}{A_i} \right) \left( \frac{G_i}{G_{std}} \right) (f_{std}) \quad (C2)$$

Where

$G_i$	=	Mass of each gas
$G_{std}$	=	Mass of standard (Methane)
$A_i$	=	Detected area from GC/FID of each gas
$A_{std}$	=	Detected area from GC/FID of standard (Methane)

Example: To find the response factor of ethylene ( $f_{i,ethylene}$ )

When  $\%_{std} = 1$ ,  $\%_{ethylene} = 1$ ,  $Mw_{std} = 16.04$ ,  $Mw_{ethylene} = 28.05$ ,  
 $A_{std} = 2670.7311$ , and  $A_{ethylene} = 4776.0771$

$$G_{std} = (4.0220 \times 10^{-7})(1)(16.04) = 6.4521 \times 10^{-6}$$

$$G_{ethylene} = (4.0220 \times 10^{-7})(1)(28.05) = 1.1282 \times 10^{-5}$$

$$f_{ethylene} = \left( \frac{2670.7311}{4776.0771} \right) \left( \frac{1.1282 \times 10^{-5}}{6.4521 \times 10^{-6}} \right) (1) = 0.9779$$

## 2. Yield of Gas Products

**Table C1** Yield of gas components

Scope	Catalyst	Gas Products (wt%)						
		Methane	Ethylene	Ethane	Propylene	Propane	Mixed-C4	Mixed-C5
	Non-catalyst	19.41	9.56	17.37	10.21	9.36	22.04	12.06
Pore Size	Al-MCM-41	20.48	9.07	18.52	10.22	10.62	21.30	9.79
	Al-SBA-15	21.94	9.61	18.89	9.90	10.30	19.81	9.55
Pore Structure	Si-MCM-41	21.81	9.79	18.83	10.05	10.32	20.69	8.51
	Si-MCM-48	22.19	9.88	19.78	10.21	11.00	19.96	7.00
Pyrolysis Char	Untreated Char	20.61	9.21	17.31	9.75	9.64	21.28	12.20
	5 M HNO <sub>3</sub> -treated Char	19.86	8.15	16.86	8.89	9.65	20.97	15.62

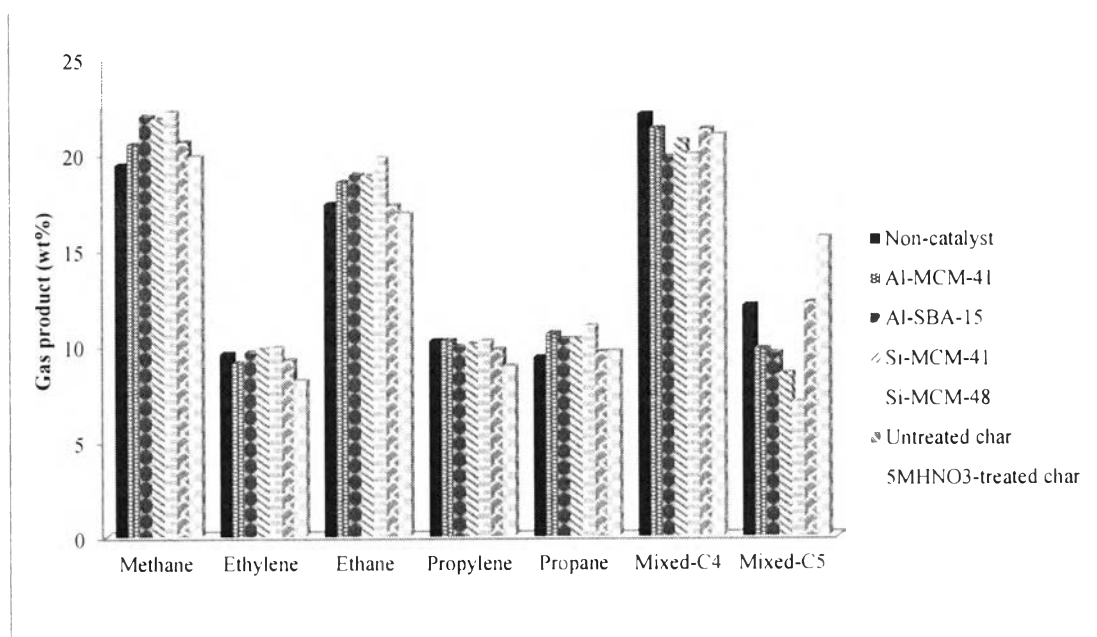


**Figure C1** Distribution of gas components.

## Appendix D Liquid Products

### 1. Petroleum Fractions (SIMDIST GC)

#### 1.1 Calibration Curve

**Table D1** Standard (ASTM D2887)

Component	Carbon no.	wt% <sup>a</sup>	RT (s)	Bp (°C)
N-hexane	6	6.0	0.660	69
N-heptane	7	6.0	1.880	98
N-octane	8	8.0	5.060	126
N-nonane	9	8.0	7.060	151
N-decane	10	12.0	8.210	174
N-undecane	11	12.0	9.140	196
N-dodecane	12	12.0	9.950	216
N-tetradecane	14	12.0	11.390	254
N-hexadecane	16	10.0	12.660	287
N-octadecane	18	5.0	13.780	316
N-eicosane	20	2.0	14.800	344
N-tetracosane	24	2.0	16.590	391
N-octacosane	28	1.0	18.110	431
N-dotriacontane	32	1.0	19.420	466
N-hexatriacontan	36	1.0	21.090	496
N-tetracontane	40	1.0	24.160	522
N-tetratetracontane	44	1.0	30.000	545

<sup>a</sup> Standard concentration

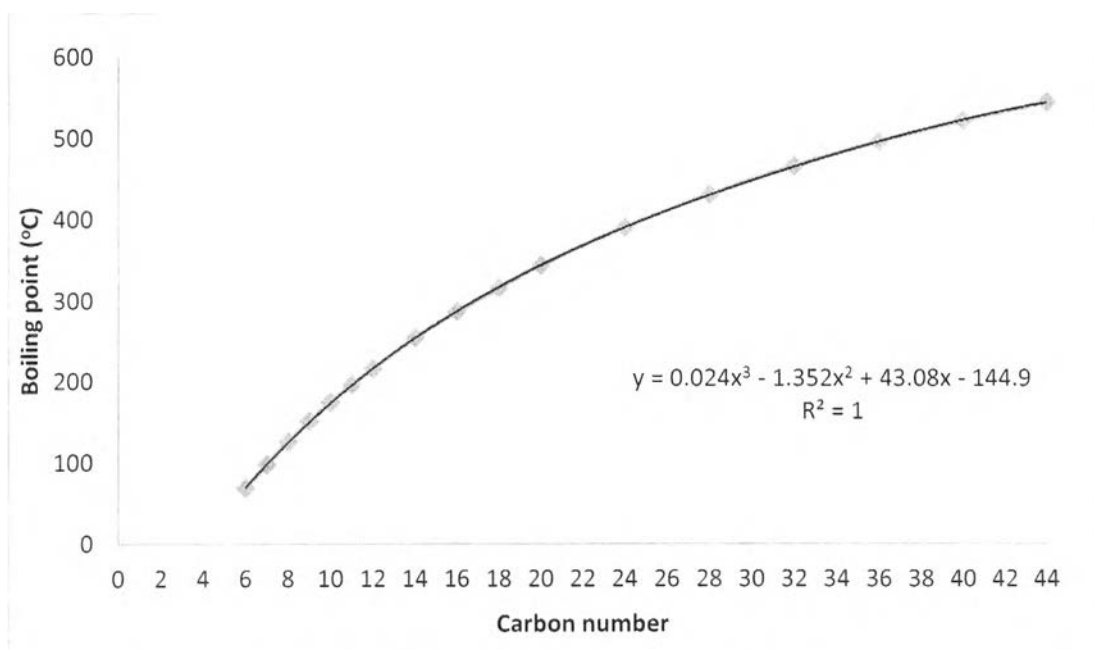


**Figure D1** Calibration curve of SIMDIST GC.

## 1.2 Petroleum Cuts

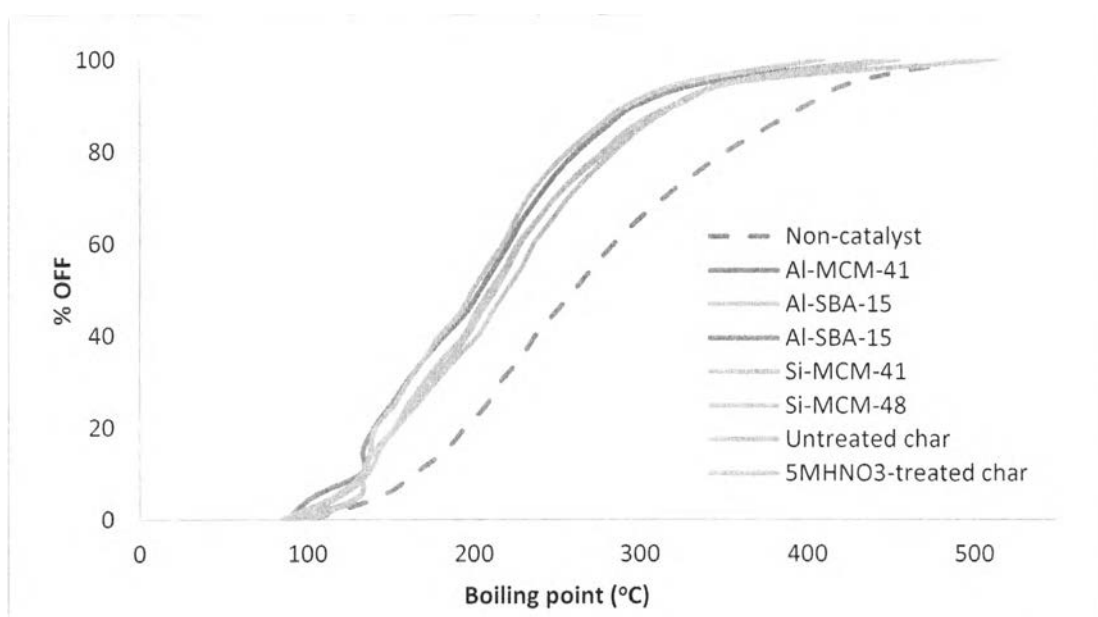


**Figure D2** Boiling point curves obtained from non-catalyst and mesoporous material case

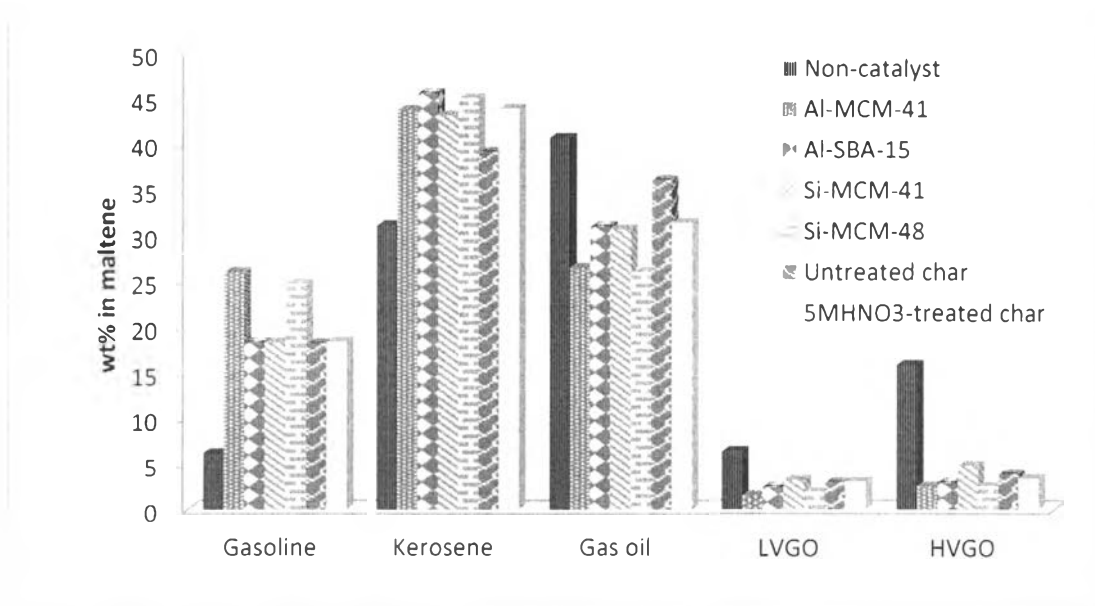
**Table D2** Influence of mesoporous materials on boiling point (°C) of maltenes

% OFF	Non-catalyst			Pore Size				Pore Structure				Pyrolysis Char			
	1	2	3	Al-MCM-41		Al-SBA-15		Si-MCM-41		Si-MCM-48		Untreated Char		5 M HNO <sub>3</sub> -treated Char	
				1	2	1	2	1	2	1	2	1	2		
0	101.4	101.2	102	87.4	80	94.8	99.6	102.4	102.4	84.9	80.4	90.9	102.3	94.8	94.8
5	132.3	136.4	143.8	103.5	103.4	130.4	131.2	131.3	131.4	115.7	108.4	119.5	131.5	130.4	130.1
10	145.5	150.4	164.3	132	131.6	132.9	132.8	132.9	134.9	133.1	132.7	136.3	135.1	132.9	132.5
15	157	162.8	182.7	132.9	132.3	139.9	139.6	139.6	141.3	137.2	135	143.2	143.9	139.9	139.9
20	167.3	169.9	194.7	139.7	138.9	152.7	152.1	152	153.1	140.8	140.1	153.4	154.7	152.7	152.9
25	173.7	185.2	207.6	149.7	146.5	163.4	161	160	164.4	152.2	148.6	165.5	166.6	163.4	166
30	187.1	195.6	216	159.5	153.3	172.1	170.4	170.1	172.3	160.3	159.3	176.8	175.1	172.1	175.7
35	195.5	206.6	228	170.1	164.8	185.7	181.3	180.8	185.6	170.1	168.6	189	187.8	185.7	190.8
40	204.6	217.1	237	182.1	172.7	195.8	193.7	193.6	196	178.8	176.3	202.3	196.8	195.8	200.3
45	214.4	225.9	249	195.1	185.3	204.1	200.6	201	205.1	191.5	188.7	210.7	205.4	204.1	209.6
50	221.4	238	260.6	203.8	195.7	213.0	208.1	209.7	215.1	199.2	197.8	219.7	214.3	213.0	218.9
55	231.1	249.4	272	212.4	204.1	220.9	217	218.9	223	208.1	207	228.9	221.1	220.9	225.8
60	240.8	262.4	284.4	221.1	212.3	228.1	223.6	226.4	232.4	217.3	216.3	236.1	228.2	228.1	236.5
65	252.7	277.3	298.3	228.7	220.6	238.2	231.6	237.6	243.7	224.4	224.1	246.7	237.8	238.2	245.2
70	265.6	292.2	314.7	238.6	228.1	248.9	241.7	249	257.8	232.5	233.2	257.1	247.3	248.9	256.5
75	280	311	332.7	249.3	238	262.1	253.5	263.4	274.1	243.4	244.9	270.1	259.6	262.1	267.7
80	300	332	352.3	262.4	249.2	278.2	266.3	280.5	289.4	257.0	260.5	285	273.9	278.2	279.4
85	329.5	356.2	375.5	278.8	263.5	294.1	282.6	297.2	309	273.2	279.2	300.5	288.9	294.1	292.5
90	374.2	392.1	399.9	298.1	283.6	319.3	300.5	323	338.2	292.3	302.1	322.7	309.8	319.3	310.2
95	438.4	444.1	428.3	341.5	320.9	355.3	335	356.9	384.9	327.9	346.2	359.6	346.9	355.3	343.1
100	500.6	500.1	497.3	448.8	437.2	446.1	432.7	454.7	474.7	410.0	422.7	513.8	436.6	446.1	437.2



**Table D3** Concentration of petroleum fractions in maltenes

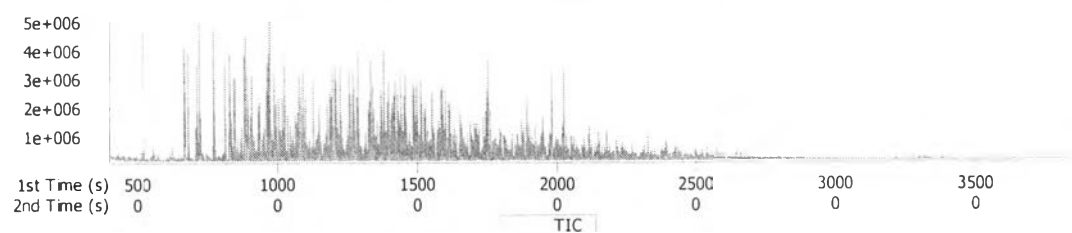
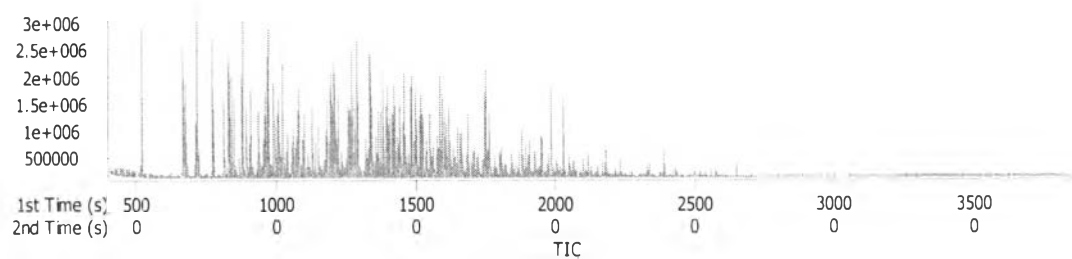
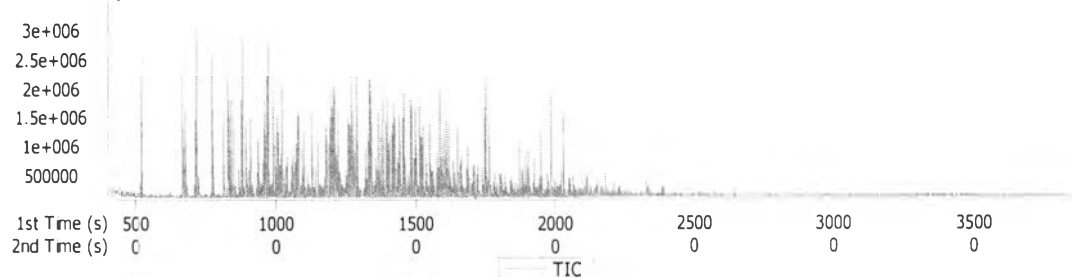
Scope	Catalyst	Petroleum Fractions (wt%)				
		Gasoline	Kerosene	Gas Oil	LVGO	HVGO
	Non-catalyst	6.18	30.98	40.55	6.36	15.93
Pore Size	Al-MCM-41	25.90	43.60	26.40	1.52	2.57
	Al-SBA-15	18.27	45.41	30.89	2.47	2.96
Pore Structure	Si-MCM-41	18.28	43.01	30.60	3.27	4.48
	Si-MCM-48	24.67	44.89	25.94	1.92	2.57
Pyrolysis Char	Untreated Char	18.17	39.00	35.93	2.98	3.93
	5 M HNO <sub>3</sub> -treated Char	18.38	43.77	31.33	3.07	3.45

**Figure D3** Concentration of petroleum fractions in maltenes.

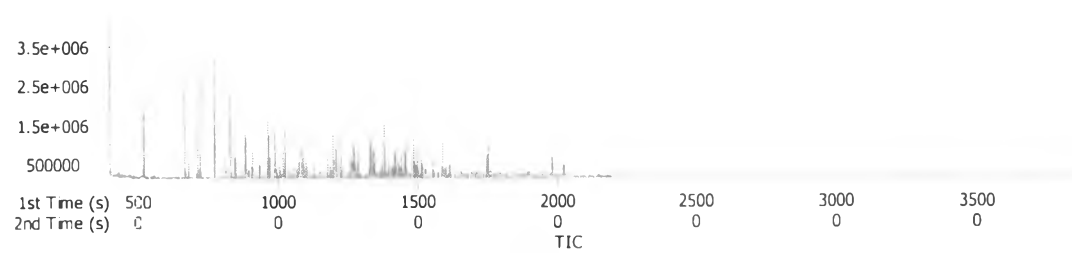
## 2. Chemical Components (GCxGC/TOF-MS)

### 2.1 Chromatogram

#### Non-catalyst I



#### Al-MCM-41



#### Al-SBA-15

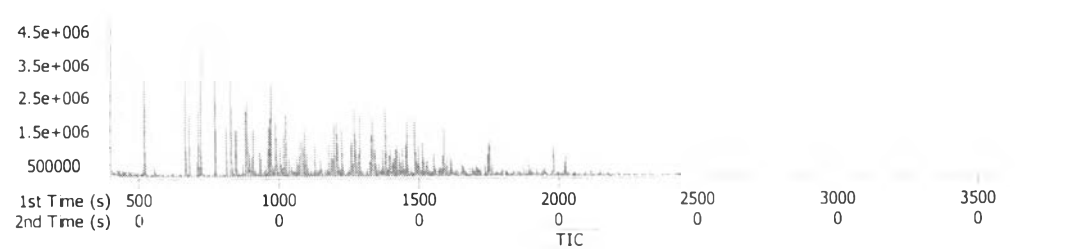
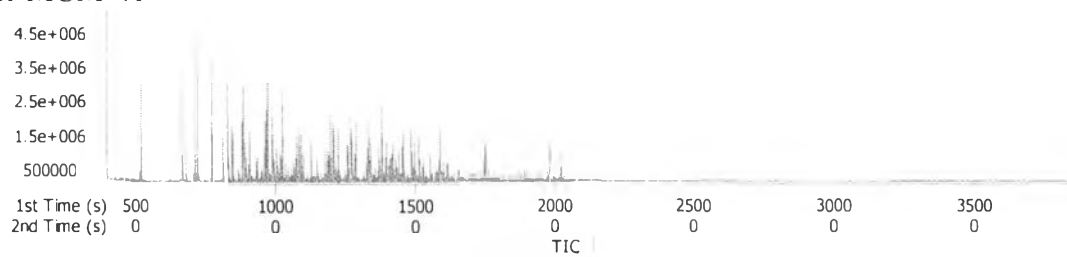
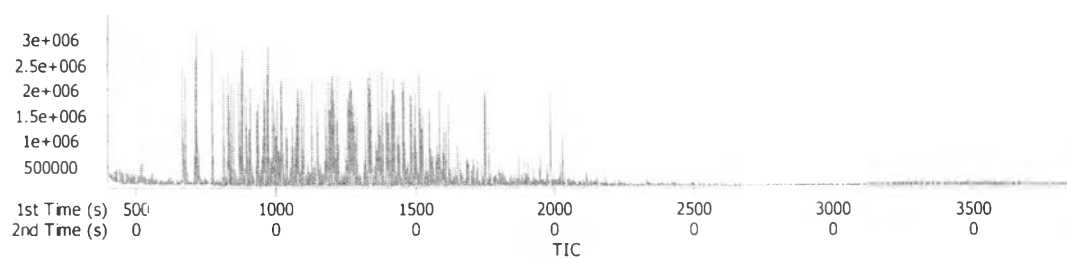


**Figure D4-1** Chromatograms obtained from pyrolysis process.

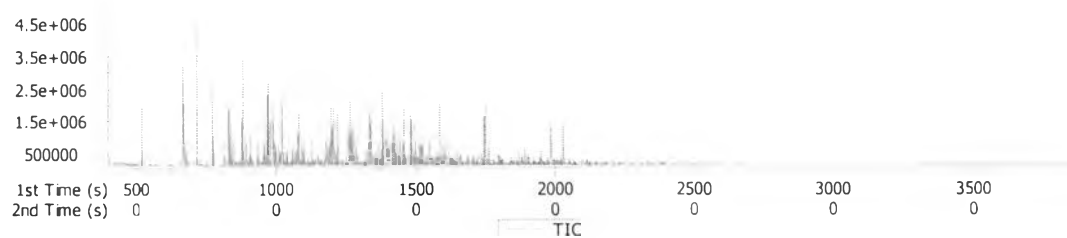
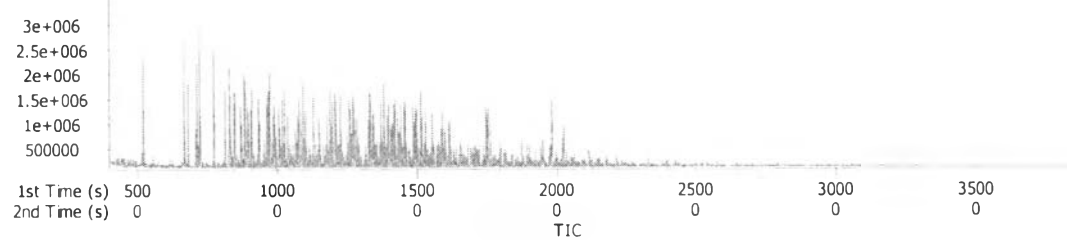
## Si-MCM-41



## Si-MCM-48



## Untreated char

5MHNO<sub>3</sub>-treated char

**Figure D4-2** Chromatograms obtained from pyrolysis process (countinue).

## 2.2 Chemical Components in Maltenes

### 2.2.1 Distribution of Hydrocarbon Groups

**Table D4** Concentration of chemical components in maltenes

Scope	Catalyst	Chemical Components (wt%)							
		SATs	OLEs	NAPs	TERs	MAHs	DAHs	PAHs	PPAHs
	Non-catalyst	5.37	6.81	2.03	5.93	47.69	9.37	12.26	10.54
Pore Size	Al-MCM-41	5.53	7.42	3.13	6.56	59.09	4.01	8.49	5.76
	Al-SBA-15	4.95	10.59	4.15	8.89	53.36	4.11	6.87	7.08
Pore Structure	Si-MCM-41	4.80	9.39	3.68	10.12	55.40	3.54	8.37	4.70
	Si-MCM-48	3.85	8.03	3.81	11.35	57.07	3.65	6.30	5.95
Pyrolysis Char	Untreated Char	4.67	8.03	4.27	8.84	52.54	4.69	9.18	7.78
	5 M HNO <sub>3</sub> -treated Char	4.05	9.38	3.19	10.56	53.54	3.07	8.52	7.69

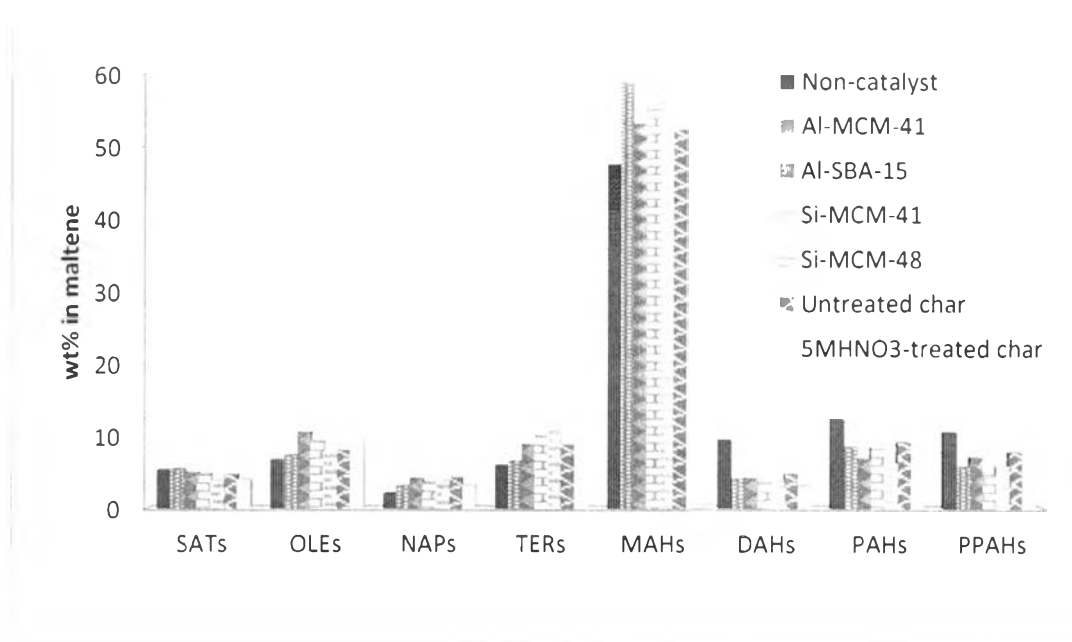


**Figure D5** Chemical components in maltenes.

## 2.2.1 Distribution of Petrochemical Products

**Table D5** Yield of petrochemicals in maltenes

Scope	Catalyst	Petrochemical Products in Maltenes (wt%)						
		Benzene	Toluene	Ethyl benzene	Mixed-xylenes	Styrene	Cumene	Total
	Non-catalyst	0.00	0.00	1.50	0.19	0.52	0.18	2.39
Pore Size	Al-MCM-41	0.00	1.80	4.57	1.37	0.09	2.28	10.11
	Al-SBA-15	0.00	0.56	3.30	0.78	0.75	1.38	6.78
Pore Structure	Si-MCM-41	0.00	0.93	2.41	0.72	0.04	1.72	5.81
	Si-MCM-48	0.32	0.77	0.85	0.86	2.18	1.72	6.70
Pyrolysis Char	Untreated Char	0.00	1.23	4.53	0.56	0.18	1.08	7.58
	5 M HNO <sub>3</sub> -treated Char	0.00	0.11	2.26	0.87	0.20	0.75	4.19

**Table D6** Yield of petrochemicals in mono-aromatics

Scope	Catalyst	Petrochemical Products in Mono-aromatics (%)						
		Benzene	Toluene	Ethyl benzene	Mixed-xylenes	Styrene	Cumene	Others
	Non-catalyst	0.00	0.00	3.14	0.39	1.09	0.39	94.99
Pore Size	Al-MCM-41	0.00	3.05	7.74	2.31	0.15	3.86	82.90
	Al-SBA-15	0.00	1.04	6.18	1.47	1.40	2.61	87.29
Pore Structure	Si-MCM-41	0.00	1.68	4.35	1.30	0.07	3.10	89.51
	Si-MCM-48	0.55	1.34	1.50	1.50	3.83	3.02	88.26
Pyrolysis Char	Untreated Char	0.00	2.34	8.62	1.06	0.34	2.05	85.60
	5 M HNO <sub>3</sub> -treated Char	0.00	0.20	4.21	1.63	0.38	1.40	92.17

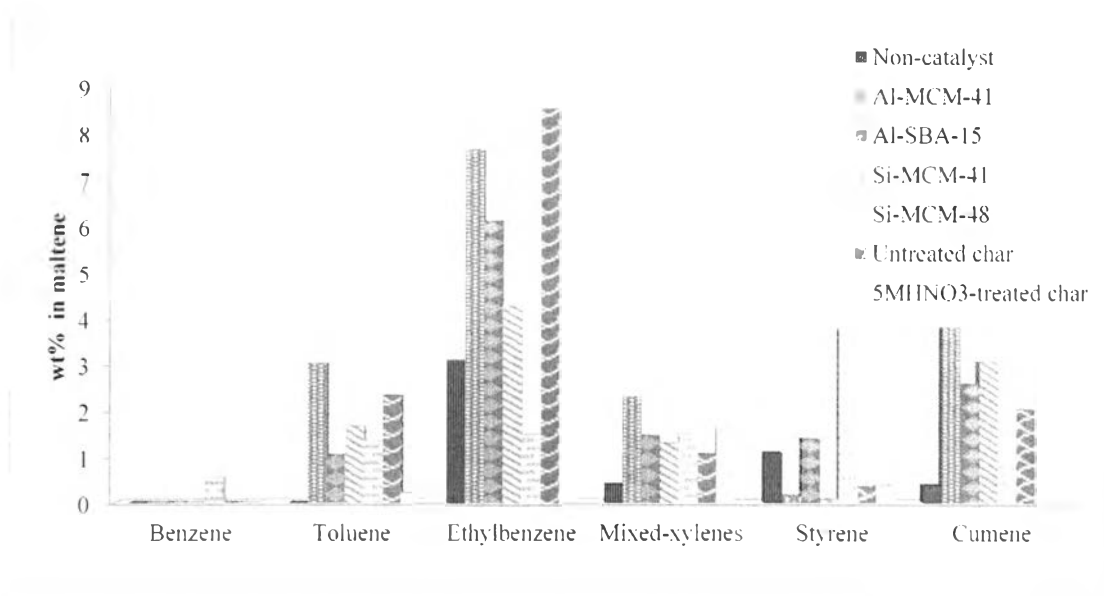


**Figure D6** Petrochemical products in mono-aromatics.

### 2.2.3 Quantification of some Petrochemical Products in Maltene Solution

The external standard (PIANO, Spectrum Quality Standards, Ltd.) was used for quantification of some petrochemical products (BTEXC). The average peak area of BTEXC, detected from GCxGC/TOF-MS, is reported in Table D7.

**Table D7** Average peak area of some petrochemical products (BTEXC) in PIANO standard detected from GCxGC/TOF-MS

Components	Concentration <sup>a</sup> (wt%)	Avg. Peak Area <sup>b</sup>	Avg. Peak Area Percentage (%) <sup>c</sup>
Benzene	2.425	4,359,114	1.713
Toluene	2.576	3,263,826	1.288
Ethylbenzene	2.504	7,726,809	3.050
p-xylene	3.374	6,955,656	2.754
Cumene	1.864	6,241,609	2.459

<sup>a</sup> PIANO standard (known concentration) and <sup>b,c</sup> GCxGC/TOF-MS (detected)

The quantification of some petrochemical products is shown in Eq. (D1) where [STD],  $A_{STD}$ , and  $A_{comp}$  are defined as known concentration of PIANO standard (wt%), average peak area percentage of standard detected from GCxGC/TOF-MS (%), and peak area percentage of component detected from GCxGC/TOF-MS (%), respectively. The concentration of petrochemical products in maltene solution is reported in Table D8.

$$\text{Component Concentration (wt\%)} = \frac{A_{comp}[STD]}{10A_{STD}} \quad (3.2)$$

Example: To determine the concentration of ethylbenzene

when  $A_{ethylbenzene} = 1.498\%$ ,  $[STD]_{ethylbenzene} = 2.504\text{ wt\%}$ ,  $A_{STD,ethylbenzene} = 3.050\%$

$$\text{Component Concentration (wt\%)} = \frac{(1.498)(2.504)}{10(3.050)} = 0.12\text{ wt\%}$$

**Table D8** Concentration of petrochemical products in maltenes

Scope	Catalyst	Concentration of Petrochemical Products in Maltenes (wt%)					
		Benzene	Toluene	Ethyl benzene	p-xylenes	Cumene	Total
	Non-catalyst	0.00	0.00	0.12	0.00	0.01	0.14
Pore Size	Al-MCM-41	0.00	0.36	0.38	0.11	0.17	1.01
	Al-SBA-15	0.00	0.11	0.27	0.00	0.11	0.49
Pore Structure	Si-MCM-41	0.00	0.19	0.20	0.00	0.13	0.52
	Si-MCM-48	0.04	0.15	0.07	0.00	0.13	0.40
Pyrolysis Char	Untreated Char	0.00	0.25	0.37	0.00	0.08	0.70
	5 M HNO <sub>3</sub> -treated Char	0.00	0.02	0.19	0.01	0.06	0.27

## 2.2.4 Petroleum fraction obtained from GCxGC/TOF-MS

**Table D9** Influence of mesoporous materials on petroleum fractions (wt%) in maltenes using GCxGC/TOF-MS

Scope	Catalyst	Petroleum Fractions (wt%) <sup>a</sup>				
		Gasoline	Kerosene	Gas Oil	LVGO	HVGO
	Non-catalyst	4.87	51.08	39.07	3.17	1.82
Pore	Si-MCM-41	9.36	59.92	28.62	1.16	0.93
Structure	Si-MCM-48	9.37	61.10	26.42	2.21	0.54

<sup>a</sup> The boiling point of sampling species was referred to the published data from Royal Society of Chemistry, 2015. Then, each of boiling points of the representative species were arranged in order to estimate the petroleum fractions.



## Appendix E Solid Products

### 1. Total Acidity of Char Sample

Char sample was firstly test the excess base, titrated with 0.1 M HCl, by using back-titration method. Then, the amount of titrant,  $V_{\text{HCl}}$ , was used to determined the total acidity using Eq. (E1).

$$\text{Acidity} = \frac{[\text{HCl}] \times V_{\text{HCl}}}{m} \quad (\text{E1})$$

Where

[HC] = Concentration of hydrochloric acid (mol/L)

$V_{\text{HCl}}$  = Volume of HCl (L)

m = Mass of char sample (g)

Example: To calculate of acidity of pyrolysis char using Eq. (E1)

When [HCl] = 0.1 mol/L,  $V_{\text{HCl}} = 12.5 \times 10^{-3}$  L,  $m = 0.1011/4 = 0.0253$  g

$$\text{Acidity} = \frac{0.1 \times 12.5 \times 10^{-3}}{0.0253} = 49.46 \text{ mmol/g}$$

**Table E1** Total acidity of pyrolysis char

Sample	Sample Mass (g)	Volume of HCl (mL)			Total Acidity (mmol/g)
		1	2	3	
Untreated Char	0.1011	12.5	12.6	12.8	49.98 ± 0.60
5MHNO <sub>3</sub> -treated Char	0.1011	12.7	12.6	12.8	50.25 ± 0.40

## 2. Elemental Contents in Pyrolysis Products (CHNS analyzer)

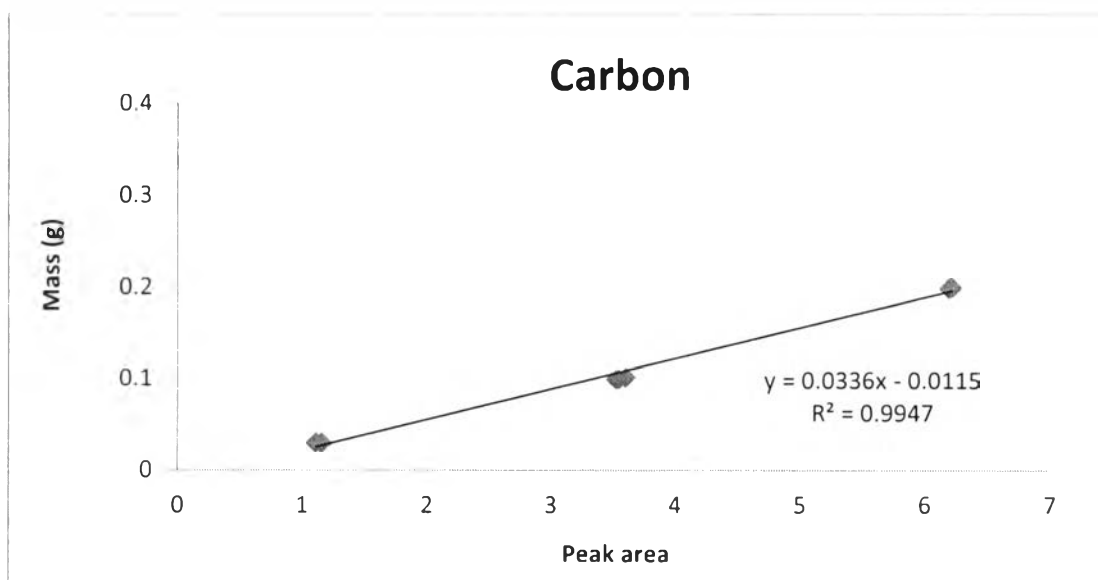
### 2.1 Calibration of CHNS Analyzer

**Table E2** Standard of CHNS analysis

Standard	Elemental Contents
EDTA (Part no. 502-092)	Carbon = $41.08 \pm 0.01$ % Hydrogen = $5.54 \pm 0.02$ % Nitrogen = $9.56 \pm 0.02$ %
Coal (Part no. 502-671)	Sulfur = $1.01 \pm 0.09$ % Ash = $9.33 \pm 0.15$ %

**Table E3** Calibration of carbon using EDTA standard

No.	Mass (g)	Certified	Calculated	Error (%)	Prev Err (%)	Peak	Peak Area	Weighting (g)
1	0.0306	41.0000	39.6530	-3.4740	-3.4740	6114.1000	1.1600	0.7966
2	0.0303	41.0000	39.5920	-3.6220	-3.6220	6071.6000	1.1510	0.8026
3	0.0309	41.0000	39.5960	-3.6124	-3.6124	6016.2000	1.1090	0.7875
4	0.1003	41.0000	44.0060	7.1237	7.1237	18675.0000	3.5409	0.2427
5	0.1024	41.0000	43.0930	6.8460	6.8460	19007.0000	3.6000	0.2378
6	0.1001	41.0000	43.7360	6.4047	6.4047	18544.0000	3.5209	0.2433
7	0.2005	41.0000	39.8170	-3.0740	-3.0740	32693.0000	6.2113	0.1214
8	0.2011	41.0000	39.6550	-3.4080	-3.4080	32684.0000	6.2046	0.1211
9	0.2001	41.0000	39.7720	-3.1834	-3.1834	32624.0000	6.1921	0.1217

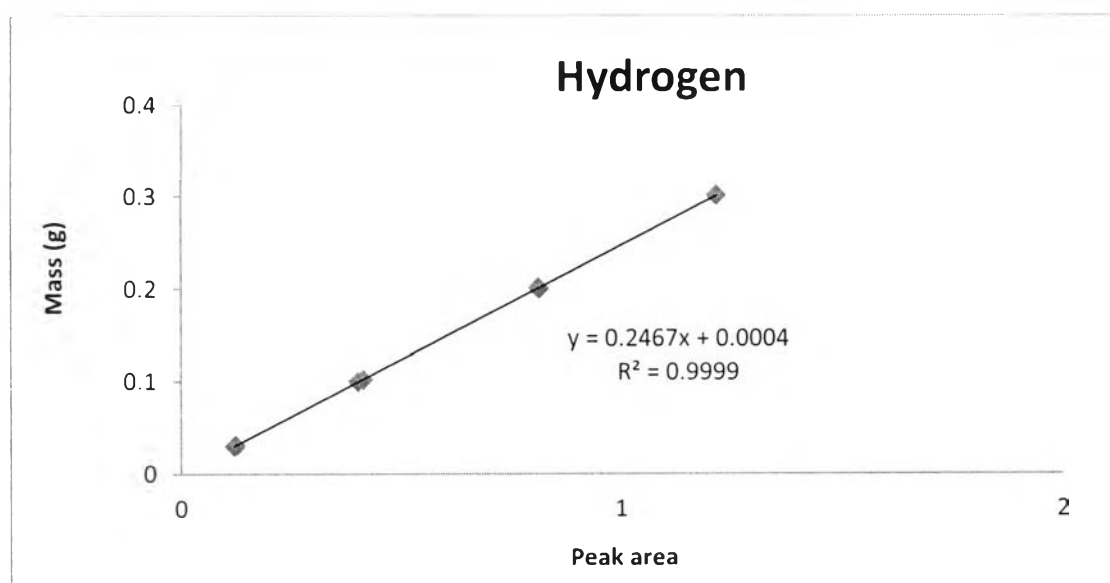


Nitrogen	Average	% Error
Calculated	40.99	1.98
Mass (g)	0.11	0.07

**Figure E1** Calibration curve of carbon.

**Table E4** Calibration of hydrogen using EDTA standard

No.	Mass (g)	Certified	Calculated	Error (%)	Prev Err (%)	Peak	Peak Area	Weighting (g)
1	0.0303	5.5400	5.5127	0.4928	0.4928	83.0740	0.1205	5.9514
2	0.0309	5.5400	5.5764	0.6562	0.6562	85.5460	0.1242	5.8397
3	0.1003	5.5400	5.5010	0.6888	0.6888	269.5600	0.4020	1.7997
4	0.1022	5.5400	5.5520	0.2318	0.2318	277.3000	0.4142	1.7629
5	0.2011	5.5400	5.5290	-0.1985	-0.1985	540.1200	0.8117	0.8977
6	0.2001	5.5400	5.5784	0.6940	0.6940	542.2600	0.8149	0.9023
7	0.3010	5.5400	5.5288	-0.2021	-0.2021	806.4200	1.2164	0.5995

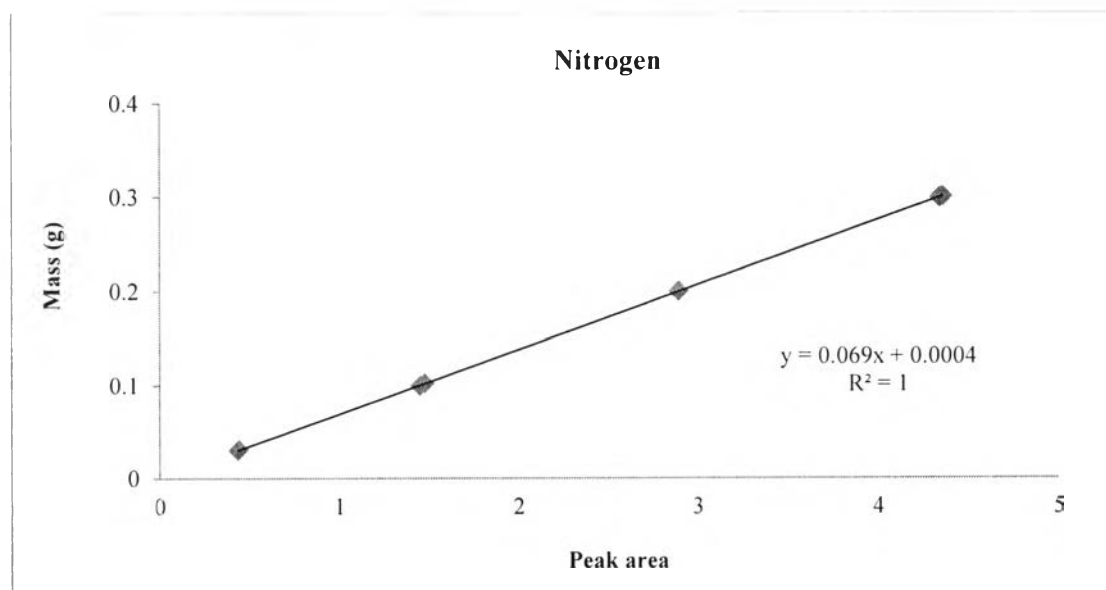


Nitrogen	Average	% Error
Calculated	5.54	0.03
Mass (g)	0.14	0.10

**Figure E2** Calibration curve of hydrogen.

**Table E5** Calibration of nitrogen using EDTA standard

No.	Mass (g)	Certified	Calculated	Error (%)	Prev Err (%)	Peak	Peak Area	Weighting (g)
1	0.0303	9.5600	9.6304	0.7364	0.7364	1.1595	0.4368	3.4488
2	0.0309	9.5600	9.4893	-0.7399	-0.7399	1.1587	0.4386	3.3841
3	0.1024	9.5600	9.5299	-0.3145	-0.3145	2.0445	1.4728	1.0216
4	0.10005	9.5600	9.6007	0.4259	0.4259	2.0187	1.4497	1.0455
5	0.2005	9.5600	9.5364	-0.2466	-0.2466	3.2611	2.8913	0.5218
6	0.2001	9.5600	9.5628	0.02888	0.0289	3.2650	2.8932	0.5229
7	0.3011	9.5600	9.5629	0.0306	0.0306	4.5172	4.3573	0.3474
8	0.3001	9.5600	9.5727	0.1327	0.1327	4.4939	4.3471	0.3486
9	0.3003	9.5600	9.5549	-0.0534	-0.0534	4.5185	4.3421	0.3483

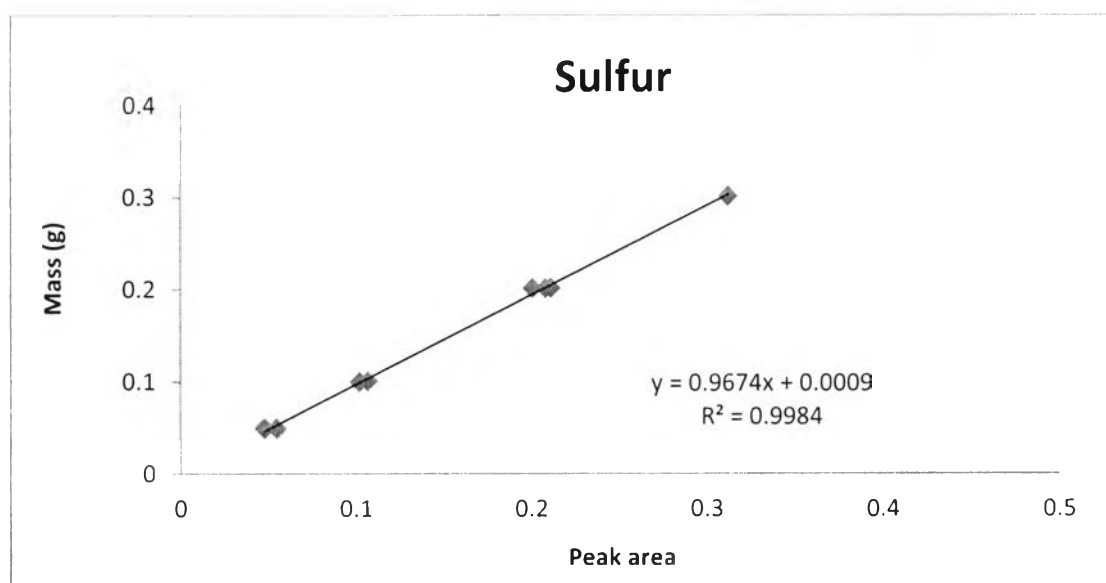


Nitrogen	Average	% Error
Calculated	9.56	0.04
Mass (g)	0.17	0.11

**Figure E3** Calibration curve of nitrogen.

**Table E6** Calibration of sulfur using Coal standard

No.	Mass (g)	Certified	Calculated	Error (%)	Prev Err (%)	Peak	Peak Area	Weighting (g)
1	0.0504	1.0100	0.9344	-7.4838	-7.4838	501.0700	0.0480	19.6370
2	0.0502	1.0100	1.0741	0.3477	0.3477	592.5400	0.0549	19.7150
3	0.1012	1.0100	1.0338	2.3590	2.3590	804.5400	0.1065	9.7865
4	0.1007	1.0100	0.9949	-1.4944	-1.4944	1043.0000	0.1020	9.8331
5	0.2016	1.0100	0.9765	-3.3210	-3.3210	1699.1000	0.2004	4.9122
6	0.2016	1.0100	1.0212	0.2095	0.2095	1120.5000	0.2078	4.9192
7	0.2025	1.0100	1.0234	1.3255	1.3255	1483.1000	0.2109	4.8906
8	0.3010	1.0100	1.0182	0.8135	0.8135	1718.3000	0.3121	3.2809



Nitrogen	Average	% Error
Calculated	1.01	0.04
Mass (g)	0.13	0.09

**Figure E4** Calibration curve of sulfur.

## 2.2 Elemental Distributions

**Table E7** Elemental contents (%) in tire-derived oils

Scope	Catalyst	C	H	N	S	C/H Ratio
	Non-catalyst	68.60 ± 1.13	9.62 ± 0.15	0.40 ± 0.04	1.27 ± 0.00	7.13
Pore Size	Al-MCM-41	61.7 ± 0.85	9.46 ± 0.21	0.52 ± 0.04	0.88 ± 0.00	6.52
	Al-SBA-15	66.25 ± 1.63	9.84 ± 0.04	0.55 ± 0.04	0.88 ± 0.00	6.75
Pore Structure	Si-MCM-41	64.75 ± 1.20	9.84 ± 0.04	0.40 ± 0.02	0.88 ± 0.03	6.58
	Si-MCM-48	61.80 ± 0.28	9.83 ± 0.24	0.34 ± 0.01	0.84 ± 0.01	6.29
Pyrolysis Char	Untreated Char	66.40 ± 1.27	9.60 ± 0.07	0.38 ± 0.04	0.93 ± 0.02	6.92
	5M HNO <sub>3</sub> -treated Char	64.40 ± 3.39	9.69 ± 0.05	0.54 ± 0.02	0.92 ± 0.00	6.65

**Table E8** Sulfur contents in pyrolysis products using mesoporous materials

Scope	Catalyst	Sulfur Distribution (wt%)			
		Oil	Spent Catalyst	Gas	Char
	Non-catalyst	25.4	0.0	19.7	54.9
Pore Size	Al-MCM-41	17.8	6.9	23.6	51.7
	Al-SBA-15	17.4	3.4	38.5	40.7
Pore Structure	Si-MCM-41	18.3	7.7	10.7	53.3
	Si-MCM-48	15.9	9.3	20.5	54.3
Pyrolysis Char	Untreated Char	18.6	1.3	25.2	54.9
	5 M HNO <sub>3</sub> -treated Char	17.3	1.1	31.7	49.9

**Table E9** Nitrogen contents in pyrolysis products using mesoporous materials

Scope	Catalyst	Nitrogen Distribution (wt%)			
		Oil	Spent Catalyst	Gas	Char
	Non-catalyst	33.8	0.0	20.1	46.1
Pore Size	Al-MCM-41	44.4	22.1	0.3	33.2
	Al-SBA-15	45.8	13.4	1.8	39.1
Pore Structure	Si-MCM-41	34.9	12.3	0.4	52.4
	Si-MCM-48	27.2	15.8	15.6	41.4
Pyrolysis Char	Untreated Char	31.9	0.1	35.5	32.4
	5 M HNO <sub>3</sub> -treated Char	42.7	0.1	23.9	33.3

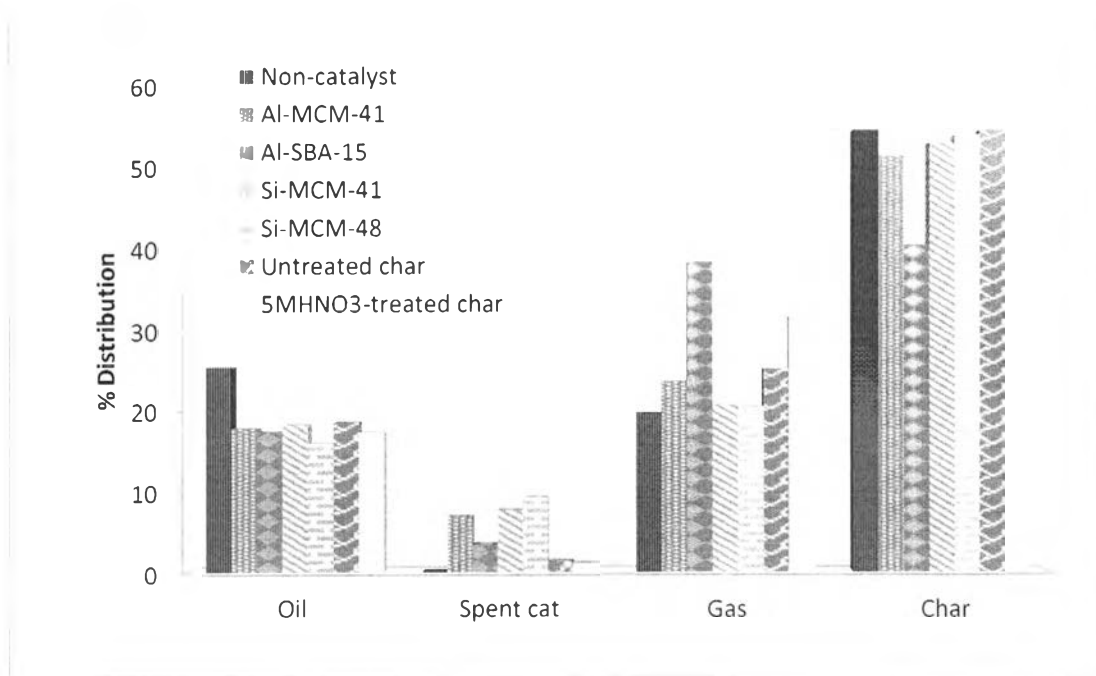


**Figure E5** Sulfur distribution in pyrolysis products obtained from waste tire-pyrolysis.

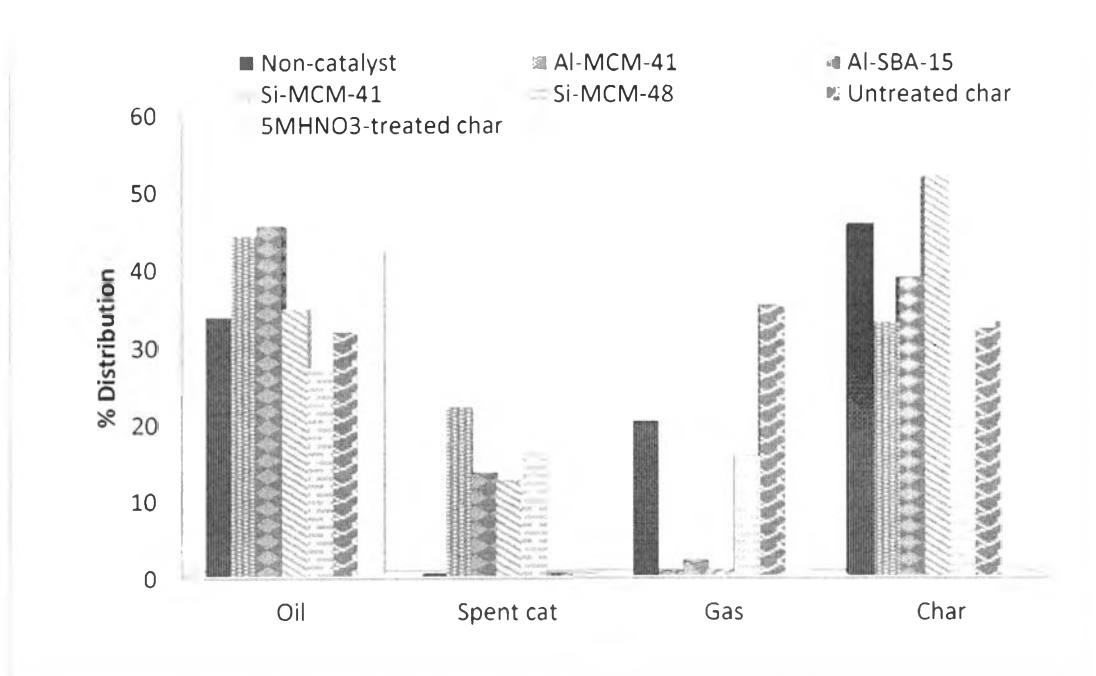


**Figure E6** Nitrogen distribution in pyrolysis products obtained from waste tire-pyrolysis.



## Appendix F Catalyst Characterizations

The general catalyst properties were analyzed using Surface Area Analyzer (SAA) and Thermogravimetric/Differential Thermal Analysis (TG/DTA) as reported in Table F1.

**Table F1** Catalyst properties

Scope	Catalyst	Pore Diameter (Å)	Pore Volume (cm <sup>3</sup> /g)	Surface Area (m <sup>2</sup> /g)	% Coke
	Non-catalyst	-	-	-	
Pore Size	Al-MCM-41	33.1	0.83	993	22.4
	Al-SBA-15	60.5	0.77	205	12.9
Pore Structure	Si-MCM-41	27.0	0.70	1,015	19.6
	Si-MCM-48	27.8	0.70	940	23.2
Pyrolysis Char	Untreated Char	229.7	0.39	70	3.7
	5 M HNO <sub>3</sub> -treated Char	255.5	0.38	96	8.3

## CURRICULUM VITAE

**Name:** Ms. Supattra Seng-eiad

**Date of Birth:** June 25, 1990

**Nationality:** Thai

**University Education:**

2009–2013 Bachelor Degree of Chemical Engineering, Faculty of Engineer, Mahidol University, Bangkok, Thailand

**Work Experience:**

April-May 2012	Position:	Student Internship
	Company name:	Asia Cement Company

**Proceedings:**

1. Seng-eiad, S.; and Jitkarnka, S. (2015, April 21) Possibility of using untreated and HNO<sub>3</sub>-treated pyrolysis char as catalysts for thermolysis of scrap rubber. Proceeding of the 6<sup>th</sup> Research Symposium on Petroleum, Petrochemicals, and Advanced Materials and the 21<sup>st</sup> PPC Symposium on Petroleum, Petrochemicals, and Polymers, Chulalongkorn University, Bangkok, Thailand.
2. Seng-eiad, S.; and Jitkarnka S. (2015, August 23 – 27) Estimation of average kinetic and maximum diameters of hydrocarbon groups in tire-derived oil for catalyst design purpose. Proceeding of the 18<sup>th</sup> Conference Process Integration, Modelling and Optimisation for Energy Saving and Pollution Reduction (PRES 2015), Kuching, Malasia. (Oral presentation).

**Extended Abstract:**

1. Seng-eiad, S.; and Jitkarnka, S. (2015, May 20-22) Identification of nitrogenous compounds in tire-derived oil using powerful GCxGC/TOF-MS for better analysis. Extended Abstract of The 5<sup>th</sup> Energy Science Technology, Karlsruhe Convention Centre, Karlsruhe, Germany. (Oral presentation).